

AIRCRAFT SCANNER DATA OVERLAY PROJECT  
STATUS REPORT

by

Paul E. Anuta

I. Introduction

A LARS data handling system development effort was started in November 1967 to solve the problem of misalignment in the aircraft scanner data being analyzed at LARS. The scanner senses visible\* wavelengths and infrared wavelengths with separate but similar detectors. This configuration results in imagery which is not geometrically coincident for all wavelengths. The initial attack on the problem resulted in a computer program which required manual alignment instructions and successfully combined visible and IR data from a flight line by December 1967. Work since January 1968 has been directed toward analysis of the data characteristics and design of an automatic system which will require no manual support once the data combination process is started. The average level of effort has been about one half time over the duration of the project.

II. Project Goals

The alignment problem arises because there are four separate sensor systems combined into the multispectral scanner system. These four subsystems detect energy in 17 channels; 1.) 80° field of view visible band - 10 channels; 2.) 80° field of view reflective infrared - 3 channels; 3.) 40° field of view reflective infrared - 3 channels; and 4.) thermal infrared, 1 channel, 40° field of view. The data from these four subsystems (also called apertures) is from the same general ground area

\* The words visible, and vis as used in this report refer to the .4 to 1.0 micron 10 channel scanner data. Infrared refers to data sensed by the scanners covering the 1.0 to 14 micron region.

but is recorded on two separate tapes. The data on the tapes is not aligned so that a particular point on the ground is represented in coincidence in all 17 channels of data. The alignment must be very exact if pattern recognition research is to be carried out based on a 17 element measurement vector for each resolution element on the target. Thus the data from the four tapes must be combined on one tape in such a manner that the data vectors have coincident information in all channels.

The alignment problem is due specifically to the fact that the data is sensed by different units, and the channels are recorded separately, digitized separately, and reformatted separately. In this process the starting points in scanner lines from different tapes may be different, sampling frequency may be different, lines may be lost on some tapes due to bad data or digitizing problems. Furthermore, the formats of the data lines are different and the angular fields of view from the apertures are different. These factors make it impossible to use the four apertures for research by addressing the tapes separately.

The research and system development work done since January 1968 has been directed toward an automated solution of this problem. The system design goals are as follows:

- 1.) (The input tapes will be referred to as the "master" and the "slave".) The first master will be the 10 channel visible band tape and the first slave will be the 1 channel thermal IR tape or a 3 channel reflective IR tape. The system will combine data from the two tapes in such a manner that data samples are coincident on the resultant data tape. For initial runs the "old" LARS 12 channel format will be used

and the IR data will replace one or more of the 12 channels of visible data. Subsequent runs will use the previous output tape as the master and the remaining IR tapes will be the subsequent slaves.

- 2.) The master and slave tapes must be manually aligned at the start of the run to within 5 lines and 5 columns of being perfectly coincident. These starting values must be punched in an input card for each run. After the run has begun the system will correlate the data and produce a combined tape automatically.
- 3.) The accuracy of the overlay process is to be plus or minus one sample and plus or minus one line from true coincidence. For the cases where an entire line of data is missing or unuseable, the system will skip the lines on the other tape to achieve coincidence.

These are the primary guidelines for the overlay system. The general topic of pictorial data analysis and processing has many aspects and there are many possible applications for techniques which can automatically extract information from pictorial data. Some applications which would be of interest to LARS researchers are:

- 1.) Automatic combination of aircraft scanner data from flight lines over the same area taken at different times. This facility would enable research to be carried out on for example June, July, and September data from the same ground resolution elements. These samples would be callable in one coincident data

vector from each ground element as the 10 data channels are presently callable. This feature would then add an additional, as well as a new, form of measurement dimension to the scanner data. The time dimension could replace a set of wavelength dimensions or the total  $NT * NC$  dimensions could in some manner be supplied to the researcher ( $NT =$  Number of times samples available for,  $NC =$  number of channels at each time).

- 2.) Boundary detection in ground areas where pictorial output display does not produce sharp border representation. The overlay system being developed performs a border enhancement process which produces a map of boundaries. This intermediate output form is what would be useful to persons doing identification of data and selection of training samples. Features which may not be recognizable at all in one or two channels can be enhanced and thereby become visible.
- 3.) Preliminary results indicate that border detection process could be used to detect areas of closely spaced changes in reflectance such as clusters of buildings. Such capability may be of value where insufficient data samples exist for training samples for small features to enable a pattern recognition technique to work.
- 4.) One border detection method being studied produces the average value for each channel in the areas outlined by the detected borders. Thus only one sample from each "field" would have to be classified by PR techniques and

and the results assigned to the total area enclosed by the border. This approach would be advantageous if the total time for border enhancement plus PR was less than for a total PR process.

The data overlay project thus has possible benefits beyond the solution of the present Michigan scanner alignment problem. The project is exploring the region of the two dimensions (spatial and temporal) not yet studied at LARS. Study of the nature and detectability of geometric shapes could be stimulated by the boundary enhancement investigation, and the availability of time as a data dimension may be of value in multispectral pattern recognition work.

### III. Data Overlay System Guidelines

The data combination requirement implies that some method is needed for correlating each sample from a visible band (or "master") aperture with each sample from an IR (or "slave") aperture. Correlation on this basis is not efficient or necessary for the scanner data problem. The misalignment problem is of such a nature that once a match is found the subsequent samples in a flight line tend to remain matched for several scanner lines. This is true since the scanners and A/D process operates with nearly identical and relatively constant parameters; i.e. shaft speed, digitization sample frequency, A/D format, etc. Thus only "small" corrections are expected for alignment and these changes should occur relatively few times during a flight line.

These factors led to the decision to correlate in two dimensions on the basis of a total scanner line and a column segment or an average of several columns. The line and column choice assumes the misalignments are purely translational at right angles to and along the flight line. Rotational distortion of the data due to aircraft yaw is not due to scanner problems and is not studied in the project to date. The basic system ground rules chosen at the start of the project are:

- 1.) Horizontal correlation on a line by line basis using all data available in the line as a range of integration. (Horizontal in the study refers to the scan line direction which is horizontal as one observes flight line printout running from the top to bottom of a page. Vertical refers to the along the flight line direction.)
- 2.) Vertical correlation using a moving segment of a column and averaging selected columns if necessary.

- 3.) Overlay is to be achieved using "checkpoints". Checkpoints are points in a flight line where a specification is made that a particular line and column in the visible or "master" data must coincide with a particular line and column of the IR or "slave" data.
- 4.) The system will execute a "three pass" process. Pass 1 will preprocess the data to enhance the features which will aid in correlation. Pass 2 will carry out cross correlation and generate a list of check points to be used in overlay. Pass 3 will combine data from two input tapes using the checkpoints from Pass 2 and write a combined data storage tape. (Future work will attempt to combine the passes for efficiency. The 3 pass approach is desirable during development. The process can be stopped and studied after each pass to see if results are acceptable to the next pass.)

The phases of the overlay process are diagrammed in Figure 1. A typical overlay configuration is shown in Figure 2. The IR data usually covers less area than the visible due to the smaller field of view thus there will be areas on the overlay tape where no IR data exists. These areas will have zero for data values. The value zero is defined as "no data" for the overlay tape and does not indicate zero data value. The value 1 will represent a data point of zero value.

The present IR scanner data covers less area than the visible and is in a sense "overlaid" on the visible. The term "overlay" is used for descriptive purposes only. The IR data is a separate channel and is not actually overlaid on but simply stored with the visible data in a correlated manner. The parameters and program variables defining the boundaries

**BORDER ENHANCEMENT PROCESS**  
DIFFERENTIATES SCANNER DATA TO  
AMPLIFY FIELD AND ROAD BOUNDRIES  
COMPUTES STEP FUNCTION CURVE FIT  
OF SCANNER DATA



**CORRELATION PROCESS**  
CROSS CORRELATES VISUAL AND  
IR/UV BAND DATA TO DETERMINE  
CORRECTION SHIFTS



**OVERLAY PROCESS**  
ALIGNS AND COMBINES DATA FROM  
VISUAL AND IR/UV TAPES TO FORM  
NEW DATA STORAGE TAPE

**FIGURE 1. DATA OVERLAY STEPS**



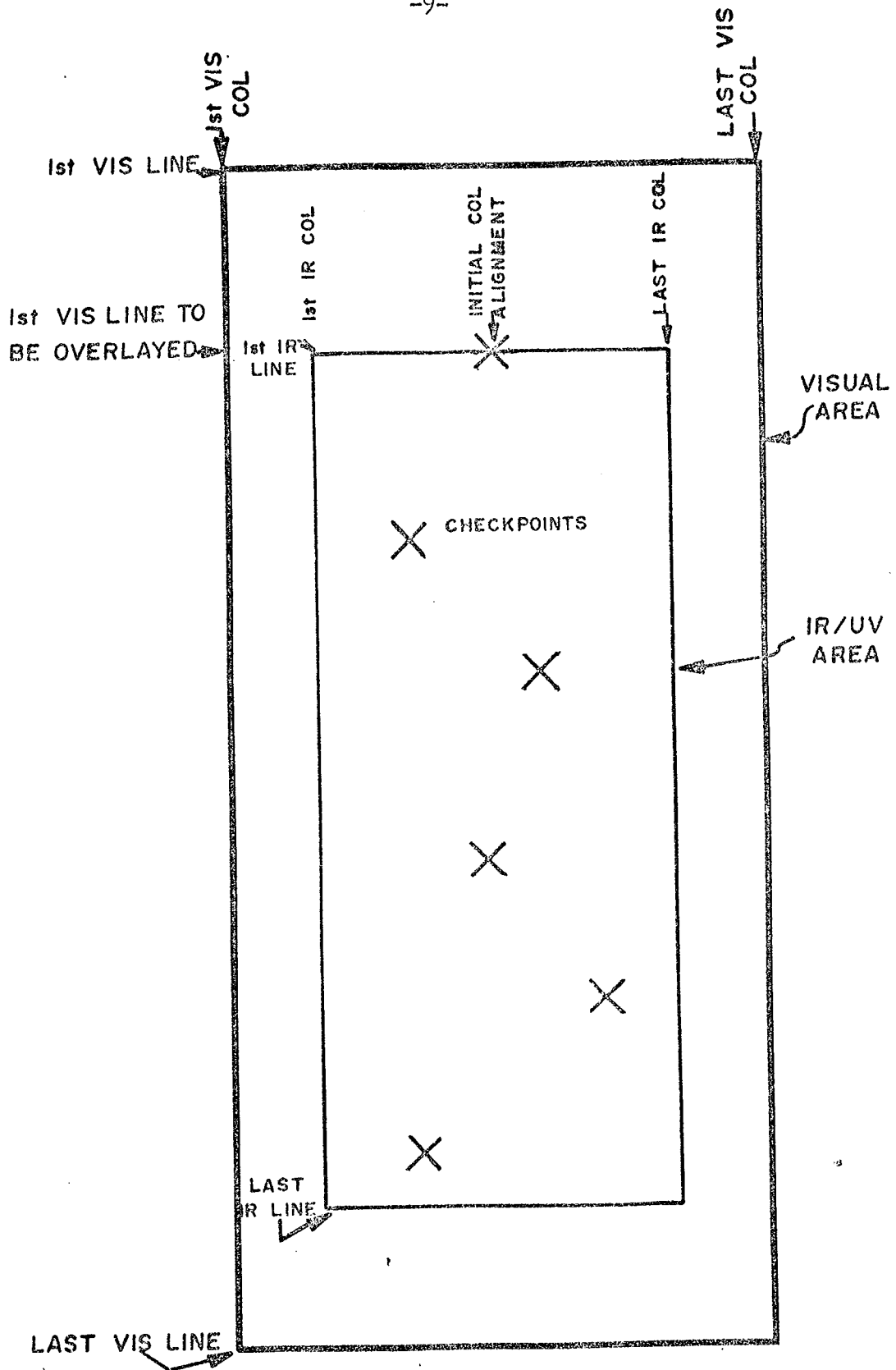


FIGURE 2. TYPICAL OVERLAY GEOMETRY

are critical to understanding the structure of the overlay operation so are discussed here:

The input data required for operation of the system is of three types: New run definition, run definition, and initial alignment. The new run definition consists of a run number for the new overlaid run to be formed the tape number to be used, and the channel the IR or "slave" data is to be placed in. Run definition consists of the run number and sample and line boundaries of the two data runs to be overlaid and channels to be used. The initial alignment data specifies the visible and IR lines and columns which will be made coincident at the start of the overlay process.

The visible run definition gives the tape line and columns specified in Figure 2 as first and last visible line and first and last visible column. The IR run definition gives the same coordinates for the limits of the area to be overlaid from the IR tape. The alignment card gives the four numbers (indicated in Figure 2 by the cross in the 1st IR line) which specify the initial alignment--this set of four numbers is essentially the first checkpoint and is treated as such in the program. Correct specification of these input data is extremely important for correct overlay and checking is done in the program to insure the specifications are at least logical. The second alignment number is the first IR line to be overlaid. This is redundant with the same item from the IR run definition since overlay cannot begin until an initial line correspondence is given. The duplication is retained arbitrarily to make the numbers complete on the cards. These data cards are all that is required to overlay data. The rest of the process is to be automatic. Thus the automatic generation of checkpoints is the basic problem to be attacked in the project. Discussion of the overlay process first is intended to form a basis for understanding the need for the data analysis work done. A brief description of what was done follows.

#### IV. Border Enhancement Experiments

The immediately obvious approach to overlaying the scanner data is to cross-correlate the unaltered data and define a match at a node in the correlation function. This was tried early in the project and results were not favorable. The basic nature of the two types of data being combined is different so that the shapes of the two data lines do not correlate in general. The similarities in the visible and IR data are geometrical and not spectral. The visible data values represent reflectance of energy whereas the thermal IR data represents emissive energy due to thermal activity in the target. A visible band area which has a high reflectance at a certain color is not necessarily at a high temperature or does not necessarily have a high emissivity. It was concluded that some means of transforming the data would be necessary in order to enhance the geometrical features of the target so that correlation could be achieved on the characteristic common to both types of data.

The target characteristic of importance is that the ground areas being observed are highly cultured; that is, man has altered the features of the land to suit his needs and in so doing has partitioned the surface so that borders are seen which did not originally exist. These borders are edges of agricultural plots, road edges, buildings, city areas and the like. These borders exist in addition to natural borders such as riverbanks and edges of forests. It became apparent that these characteristics of the target could be used to enable cross-correlation and scanner data overlay. Borders in an area will be common to data from different sensors whereas the data characteristics from areas, say within a field, may be markedly different. This notion was used as a basis of the overlay research which has been carried out at LARS. The item which was studied first was thus the border detection

problem. Several methods of preprocessing the data were investigated and a brief discussion of that work follows.

The general problem studied is that of enhancing certain attributes of scanner imagery while suppressing others. The features of particular interest here are the lines which form the boundaries between say a corn field and a wheat field or a road and a field along side it. Several methods of performing the enhancement are studied. All of the methods fall into two categories, however, those which utilize the data values and those which use the derivative of the data. The nature of the changes in reflectance and emittance of the data suggests strongly that differentiation of the image should cause borders to stand out while suppressing the data within bordered areas. Differentiation experiments constitute the major part of the work done to date; however, step function curve fitting of the unaltered data is a process which was also studied. The methods of enhancement studied in detail or briefly looked at are listed below:

- 1.) Processes Using Differentiated Data
  - a. Horizontal and vertical 1st difference
  - b. Prefiltered 1st differences
- 2.) Processes Using Data Values
  - a. Step function curve fitting
  - b. Filtering data before curve fitting

#### Differentiation of Imagery

Two factors exist which suggest that differentiating imagery will enhance borders. One is the previously indicated fact that scanner data tends to remain constant across agricultural fields and other features of

large areas and "jumps" across boundaries to new values. The second is that in some cases data is available from more than one coincident channel as in the case of the 10 channel .4 to 1.0 micron scanner used by the University of Michigan. The derivatives from the multiple channels can be combined to form a composite derivative which will accumulate the effect of borders in each channel and provide a high "contrast" border enhancement process.

The overlay requirement most extensively worked with in the project was the combination of 10 channel visible and reflective IR data with one channel thermal IR data. The visible band data enables boundary derivative accumulation by a factor of 10 whereas the thermal IR has only one channel thus a "sharp" and a "noisy" border enhancement result was expected for the two types of data, respectively. The first difference corresponds to the first derivative for discrete data. The first difference is taken of adjacent points in the horizontal and vertical dimensions in the program developed. The magnitude of the difference is summed since negative and positive differences both indicate a boundary irrespective of whether the data is increasing or decreasing in value. Also the data value may be decreasing in one channel and increasing in another at the same border and to achieve an accumulation of border indication summing of positive values is required. The operations performed are:

$$\Delta LN_{ij} = \sum_{k=1}^N |x_{i,j}^k - x_{i,j-1}^k| \quad j=2, NPTS$$

$\Delta LN_{ij}$  = 1st line difference for ith line, jth sample  
(column)

k = channel index

N = Number of channels available

i = line

j = column

$x_{ij}$  = sample value for ith line and jth column

NPTS = number of columns in line

The difference between lines for column j is:

$$\Delta CO_{ij} = \sum_{k=1}^N |x_{ij}^k - x_{i-1,j}^k|$$

$\Delta CO_{ij}$  = 1st column difference for ith line, jth column

The expressions above are implemented as part of the border enhancement phase (See Figure 1) and several flight lines of data have been processed. The horizontal (line) and vertical (column) differences are written on a data storage tape along with the sum of the two so that a complete border enhancement pictorial printout can be obtained for display purposes. The cross correlation process, however, uses the differences separately.

The effect of basic differencing on typical lines of scanner data is illustrated in Figures 3 and 4. Only plots for two lines and columns from the 1966 C1 flight line are presented. Similar plots for other flight lines studied could be presented; however, the effect is similar for all the data. The important characteristics of the differencing transformation on the data can be seen from these plots. The plots of line 141 show several interesting results of differencing. The most prominent is the high and extremely wide pulse at the center of the plot which is due to a paved county road which runs the length of the flight

line. The width of the road contributes the majority of the wide derivative span; however, a data system error effect is also present. The bright road imagery value is represented as the large negative (down-going) pulse in the center of the data value curve (upper curves in Figure 3a and c). The sharp positive pulse to the left of the road pulse is not data but is due to ringing in the scanner electronics and causes a large spurious value to be added to the derivative and causes the derivative pulse to be broadened and to peak at an erroneous point. Assuming the road is represented by a triangular pulse peaking at the center of the road, the magnitude of derivative should be a square pulse having the same width as the road. As is evident, the pulse is not square, but peaks slightly to the left of the center of the road. If correlation is carried out with imagery from another scanner, which may produce a different derivative characteristic, erroneous lockon could result. Thus system "noise" is seen to cause possible error in the overlay process.

Figures 3b and d are plots of the difference for the single channel thermal IR scanner. In Figure 3b a very large difference is seen in the received energy from the left and right sides of the road. [Note: the IR scanner has a  $40^\circ$  field of view whereas the visible band scanner has a  $80^\circ$  field of view, thus only half of the IR line has data.] From left to right, the ground cover being sensed is soybeans (data value 128) then the sharp negative step is a bare soil field (data value about 100) then on the right of the road is a wheat field. The data value rises rapidly at the right side of the bare soil field, peaks at 110 on the horizontal axis at a data value of about 170, and then settles back to the wheat field value. The derivative peaks at the steepest part of of the rise toward this data peak as is expected. At first glance, the positive peak in the IR data would presumably be the road and one might

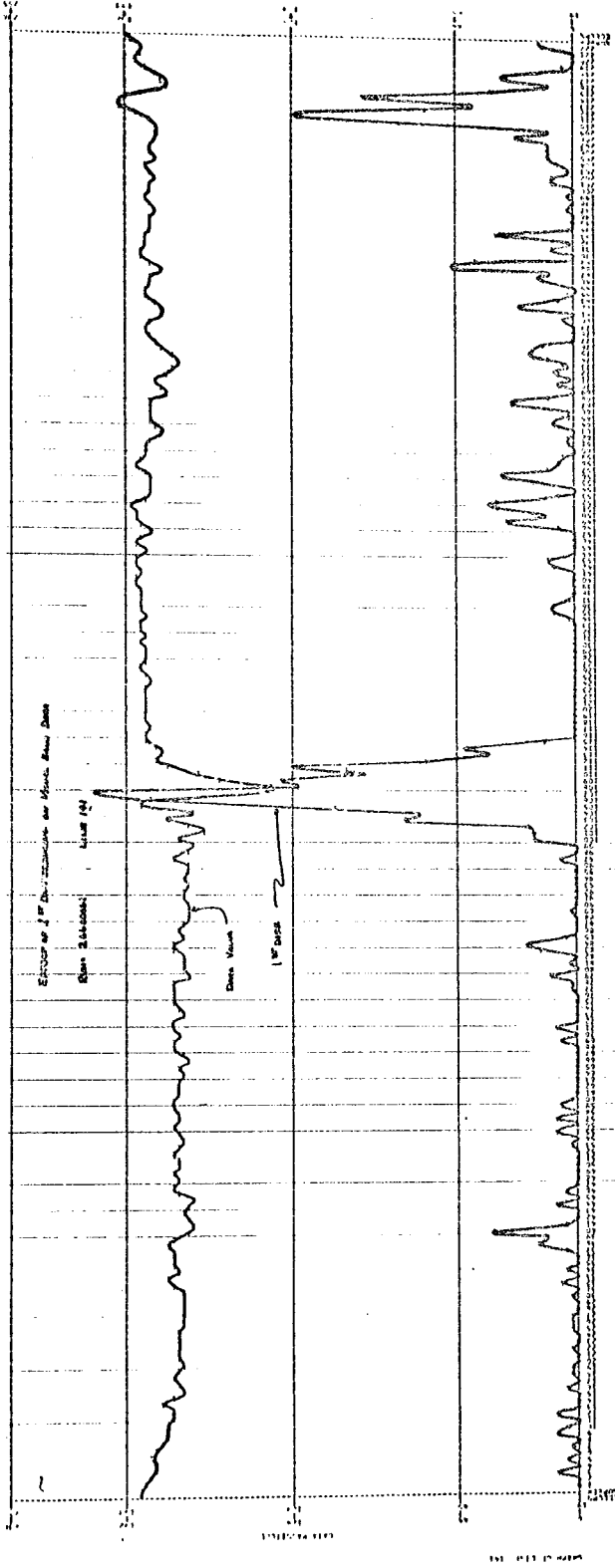


Figure 3a. First difference plot of visible band data line

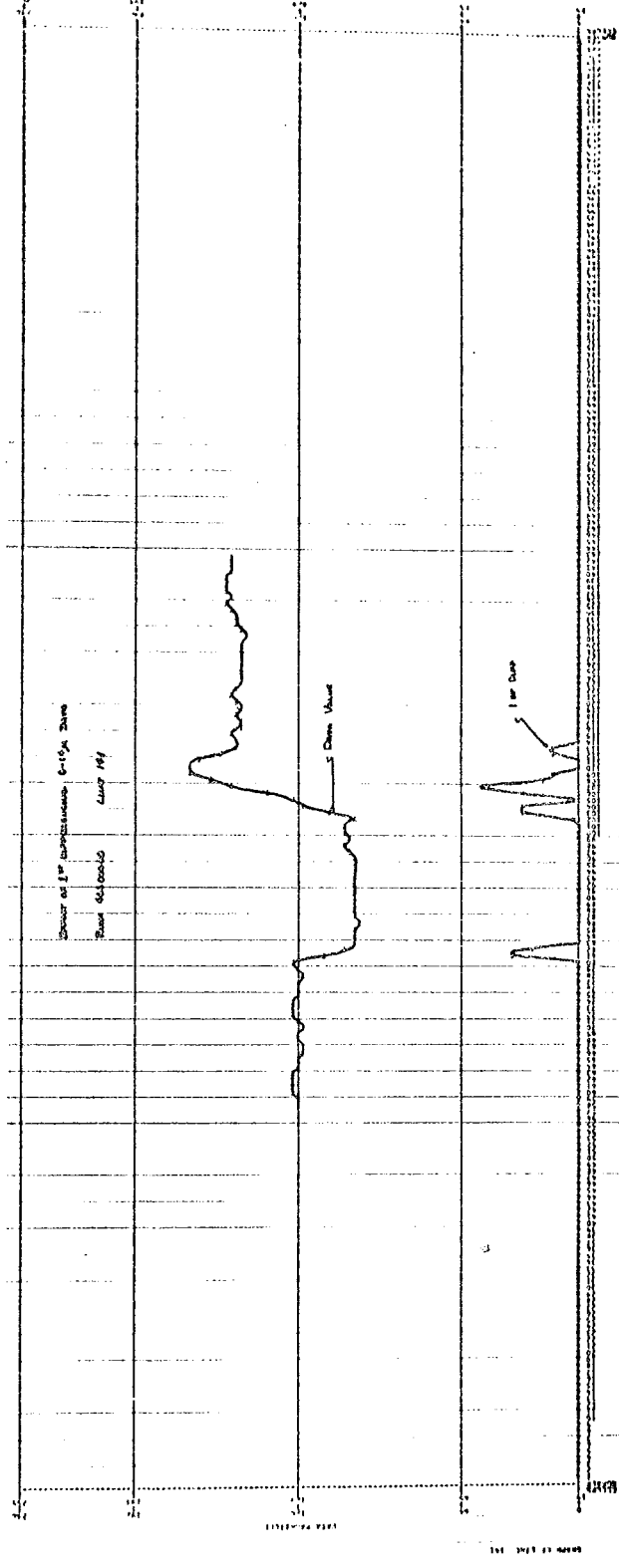


Figure 3b. First difference plot of far IR band data line



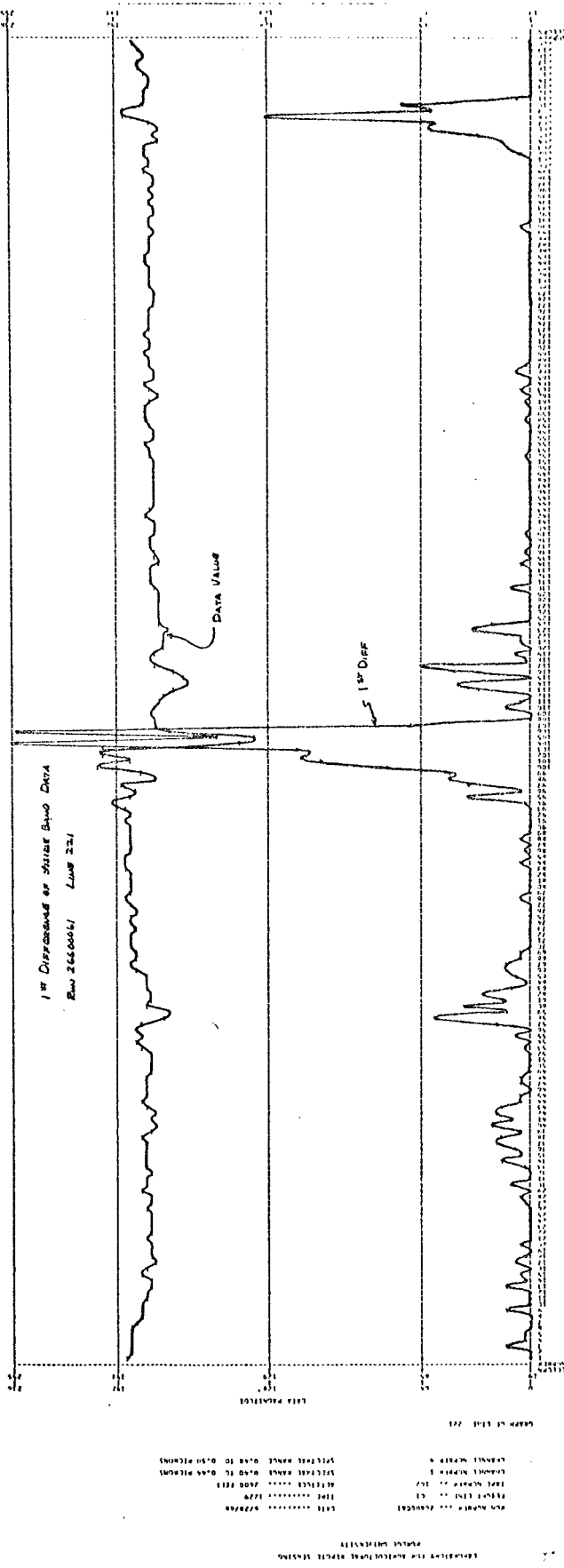


Figure 3c. First difference plot for visible band data line

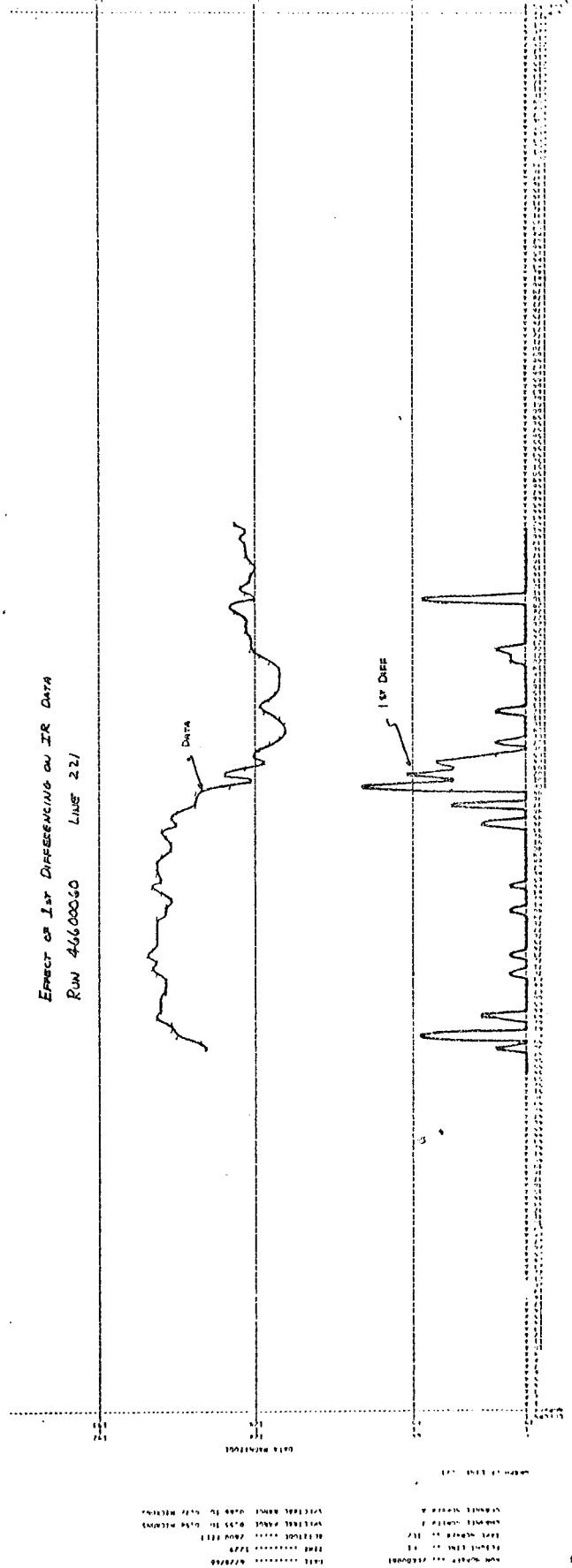


Figure 3d. First difference plot for IR band data line

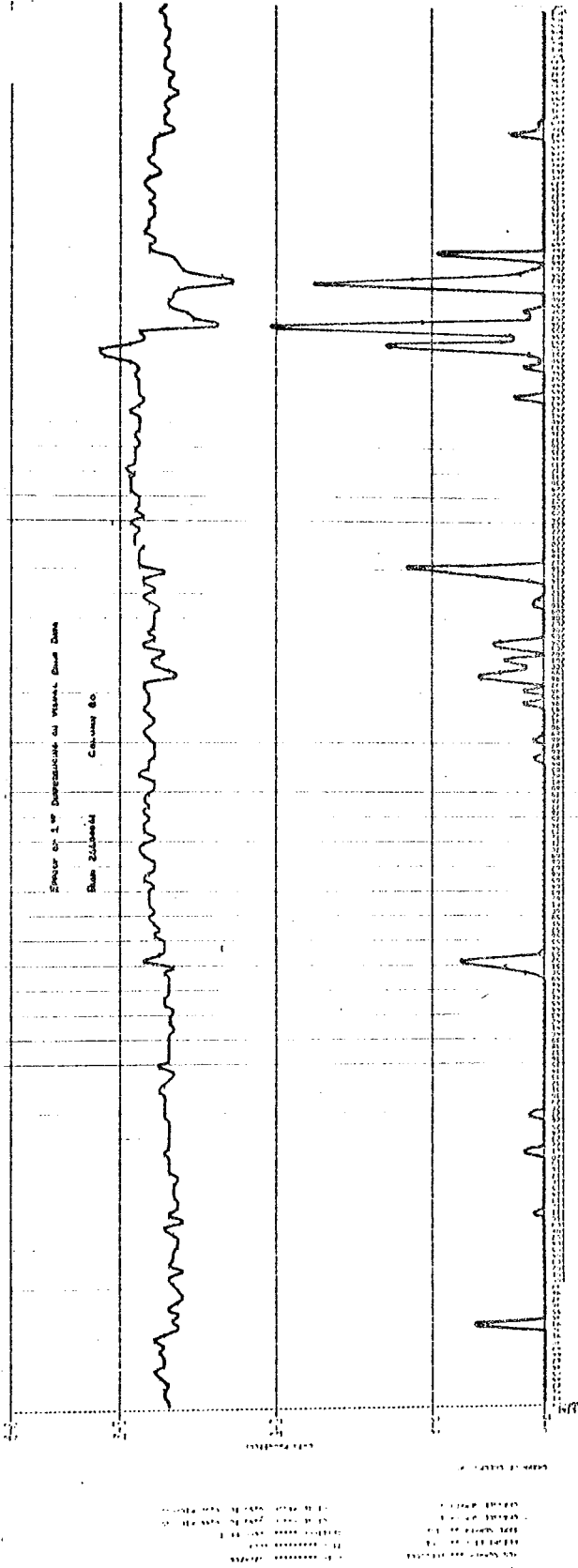


Figure 4a. First difference plot for visible band data column

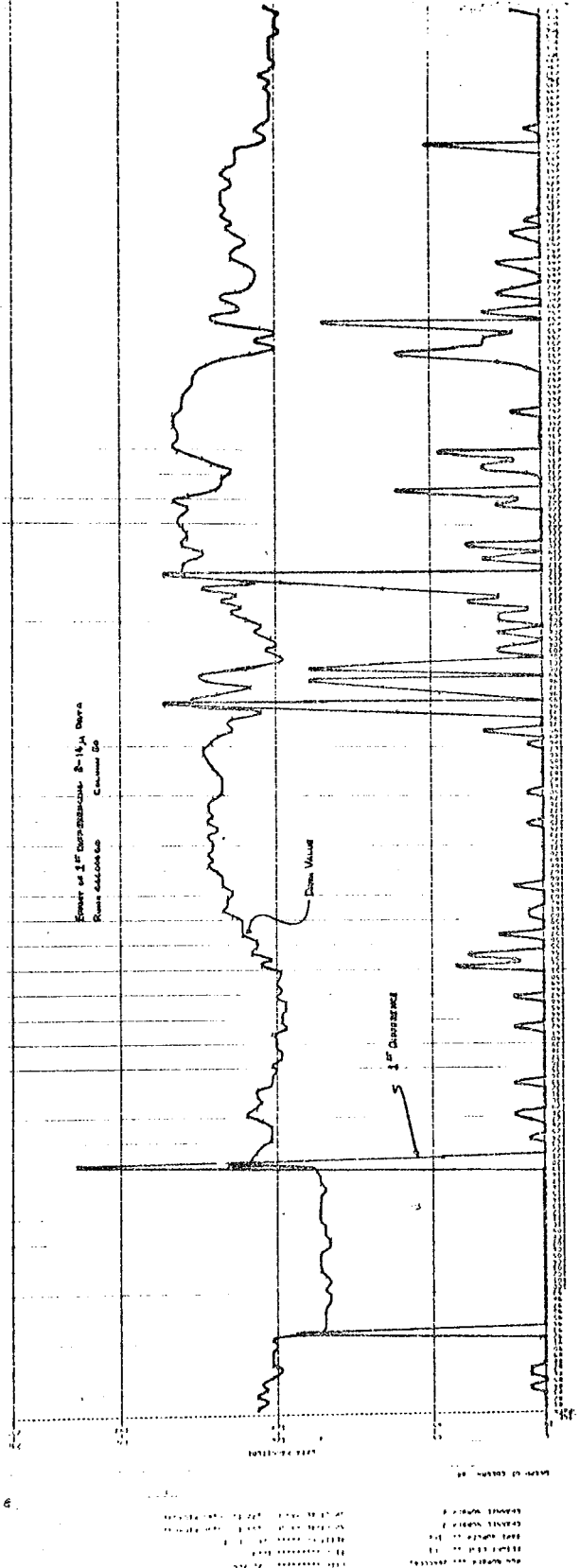


Figure 4b. First difference plot for IR band data column

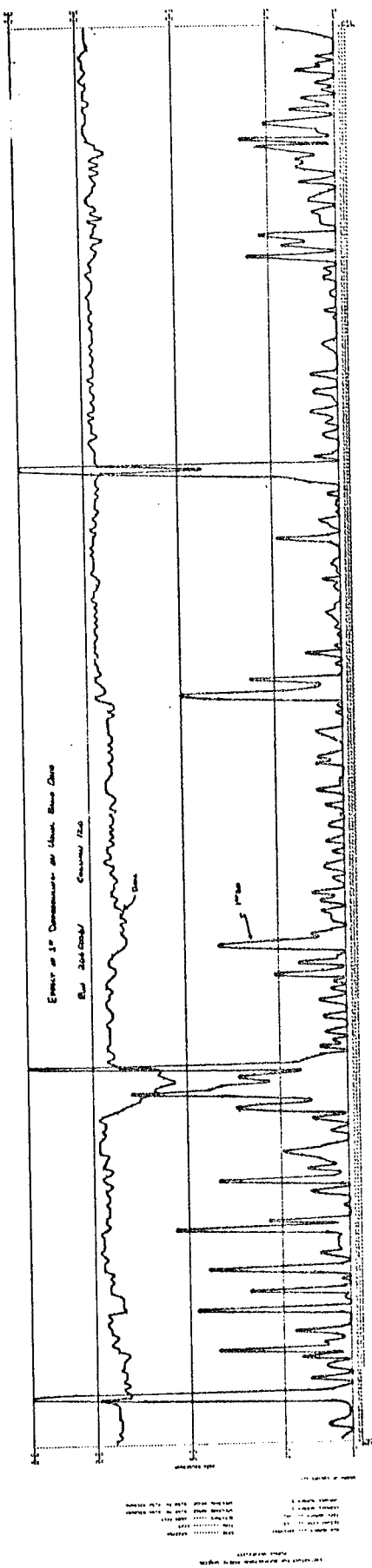


Figure 4c. First difference plot for visible band column

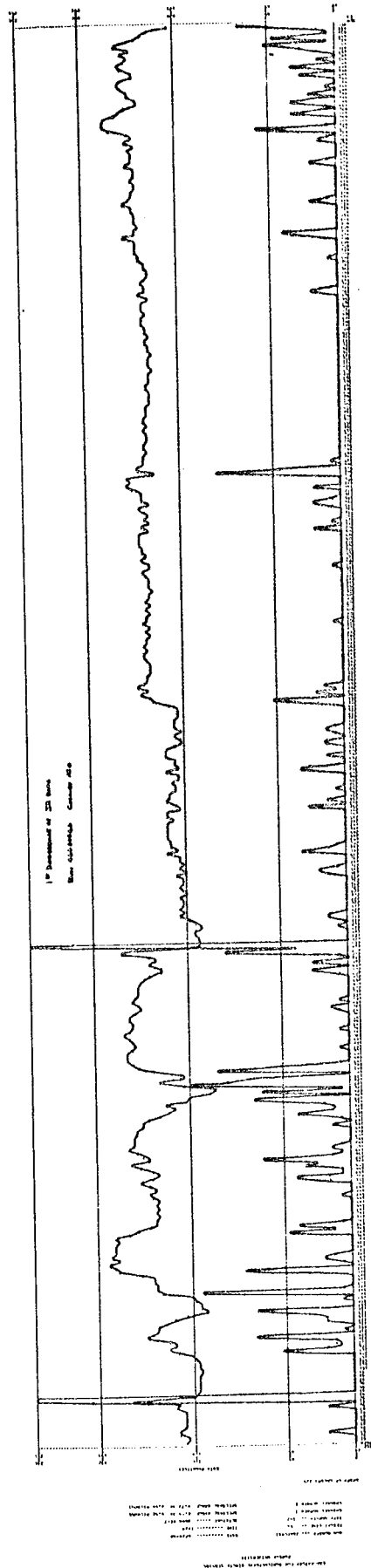


Figure 4d. First difference plot for IR band column

expect the overlay system to line up the two peaks in the data. Close examination of the rest of the IR line, pictorial printouts, and photographs of this area shows that this would not be a correct result. The left side of the bare soil field occurs at column 84 in the visible band and at column 82 in the IR. Also the center of the road is at column 107 in the visible and 105 in the IR. Thus the pulse in the IR at column 110 is not a response from the road but is a "cool"\* area along the road inside the wheat field which can be noticed in a photograph of the area. The road is, in fact, represented by a slight decrease in the slope of the IR curve at column 105 and causes a dip in the derivative curve. A completely false interpretation of the boundary information of both the data and derivative occurred by both the program and human interpreter. The point of this discussion is that neither the data or its derivative offers accurately enhanced data and steps must be taken to analyze and design an algorithm which will correctly define borders.

The first differencing approach offers a good but not a perfectly accurate method of enhancing borders - the error being due to two causes; (1), noise fluctuation in the imagery, and (2), differences in the nature of the data (i.e., reflectivity versus emissivity). In an attempt to reduce the data fluctuations which cause spurious peaks in the derivative the scanner data was preprocessed through a low pass filter and border enhancement and correlation was performed on the modified data.

#### Scanner Data Pre-Filtering Analysis

In the work carried out, two simple low pass filters were used to smooth scanner data lines only; and border enhancement and correlation

---

\* The apparent brightness or temperature of the scene increases with decreasing data value.

results were compared to the results using unfiltered data. Two linear filters were studied:

$$1. \quad y_i = \frac{X_i + X_{i-1}}{2} \quad i = 2, \text{ NPTS}$$

and

$$2. \quad y_i = \frac{X_{i-1} + X_i + X_{i+1}}{3} \quad i = 2, \text{ NPTS}$$

where  $X_i$  are the values of scanner data points and  $y_i$  the filtered values; NPTS is the number of points in a scan line. Assume  $\{X_i\}$  represents a sequence of points obtained by sampling a sinusoid:

$$X_i = e^{j\omega\Delta t i}$$

where:  $\omega$  = Frequency (radians/sec.)

$\Delta t$  = Sampling interval (sec.)

$$j = \sqrt{-1}$$

Then:

$$1. \quad y_i = e^{j\omega\Delta t i} \frac{(1 + e^{-j\omega\Delta t})}{2}$$

$$2. \quad y_i = e^{j\omega\Delta t i} \frac{(1 + e^{-j\omega\Delta t} + e^{j\omega\Delta t})}{3}$$

Assume that the data was sampled at an interval of 1 sec. Then the effect of the two filters can be predicted as a function of frequency relative to the sampling frequency. The power spectrums for the filters are given by:

$$1. \quad P_1 = \frac{1 + \cos\omega}{2}$$

$$2. \quad P_2 = \left( \frac{1 + 2 \cos\omega}{3} \right)^2 \quad (\omega = 2\pi f)$$

These two functions are shown in Figure 5a as a function of  $f_r = f/f_s$ , where  $f$  is the true frequency and  $f_s$  is the sampling frequency. The three term linear filter clearly offers significant bandwidth reduction

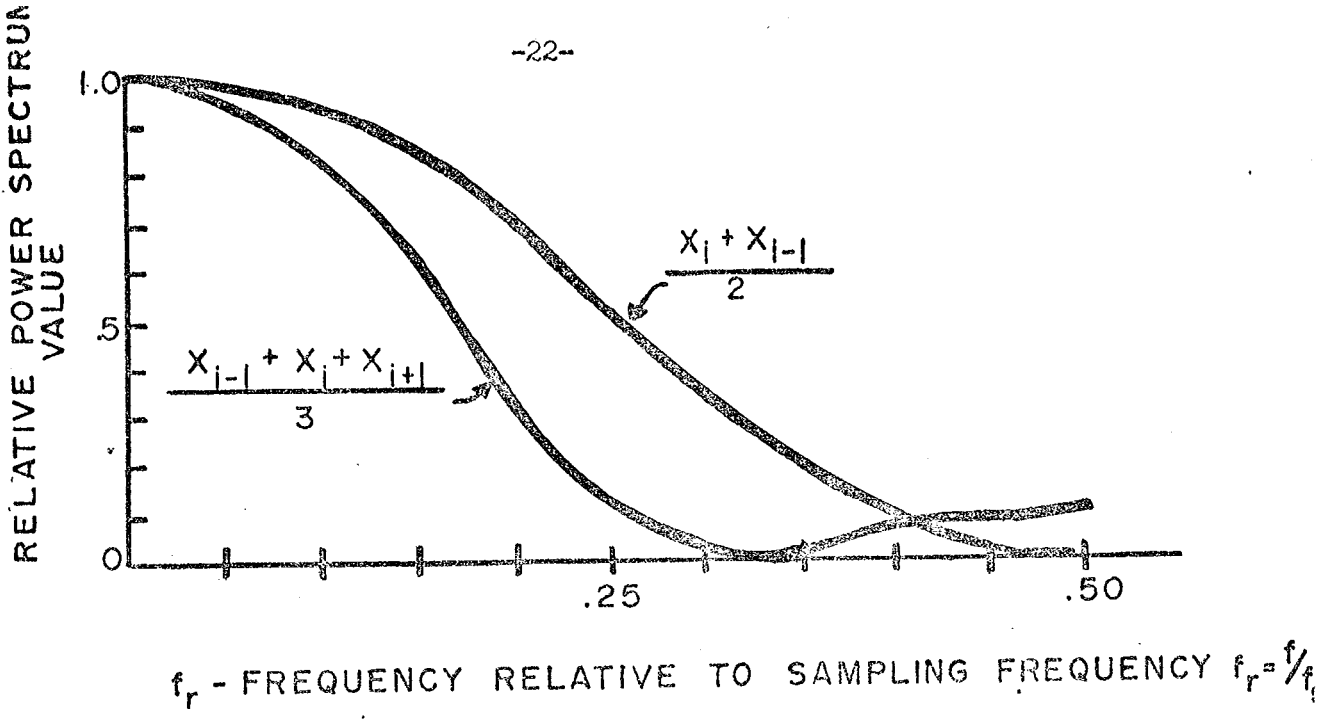


Figure 5a. Filter bandpass

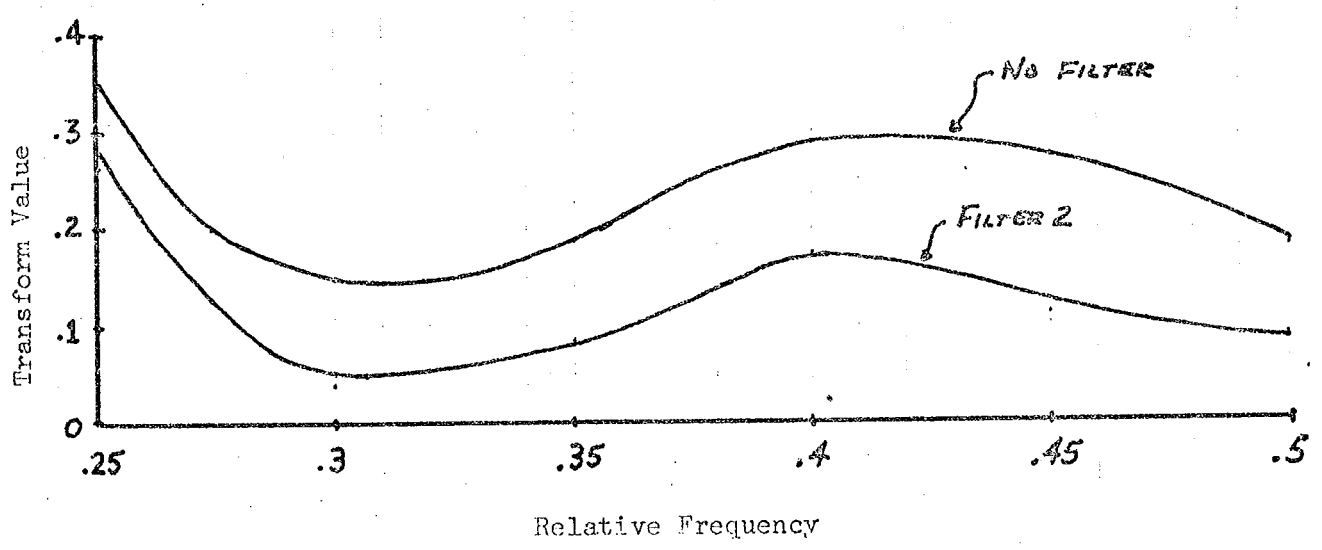


Figure 5b. Effect of filter on spectrum of visible band line 141

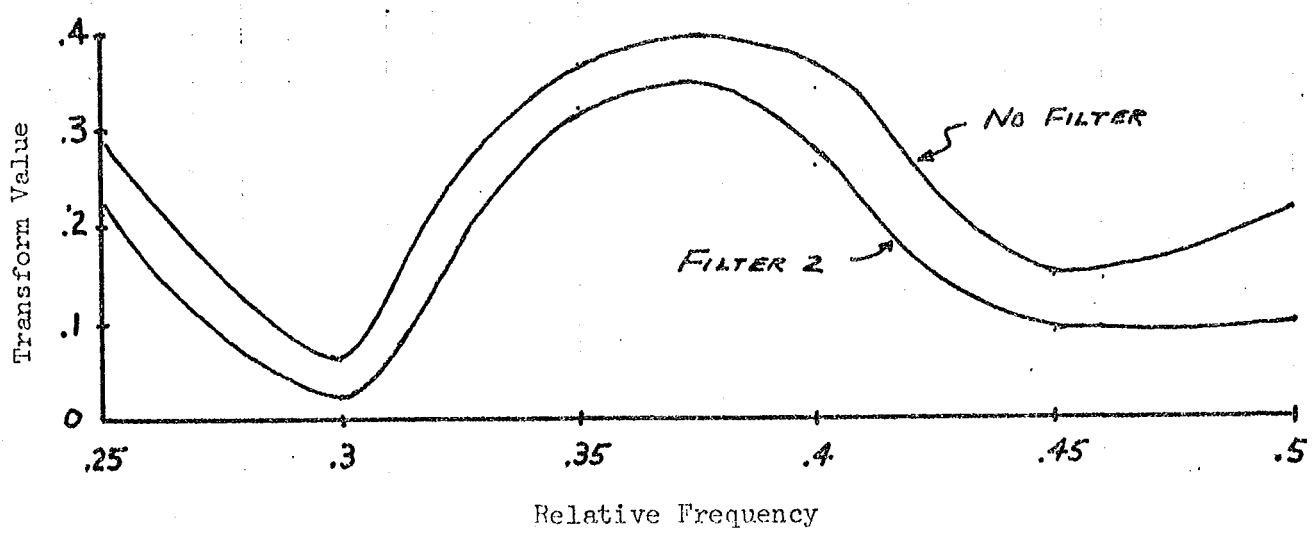


Figure 5c. Effect of filter on spectrum of IR line 141

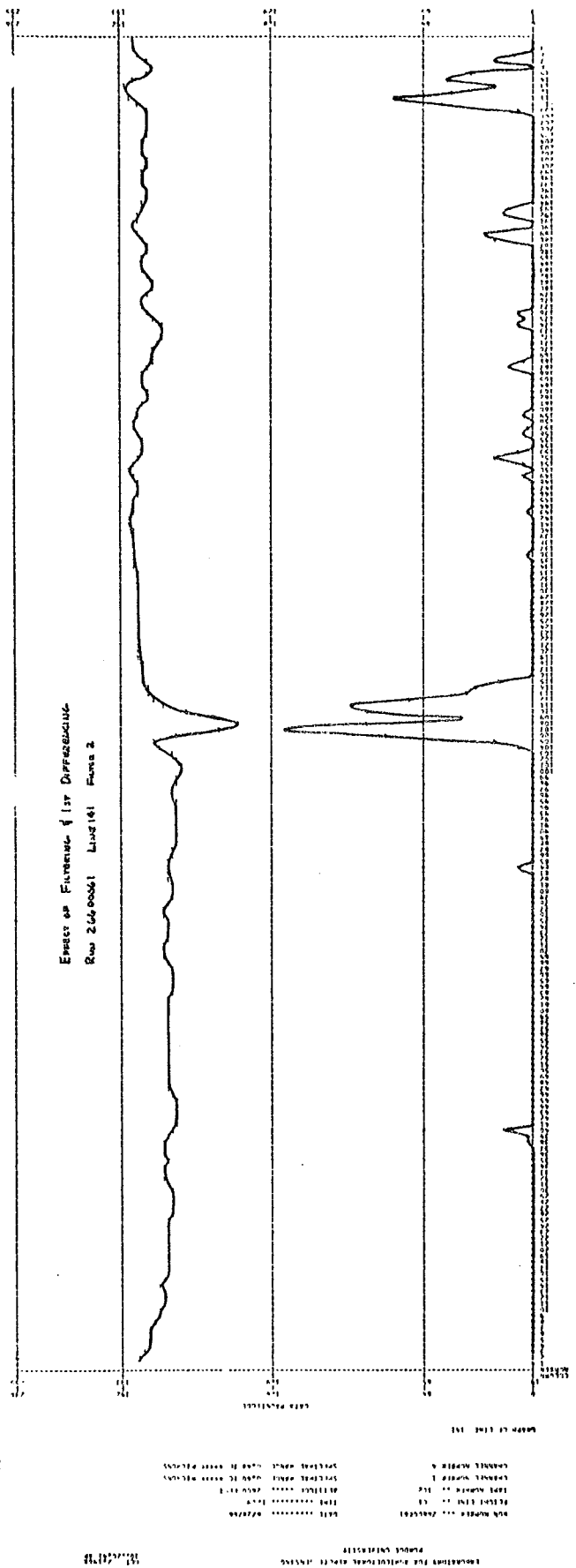


Figure 5d. Filtered vis data line 141

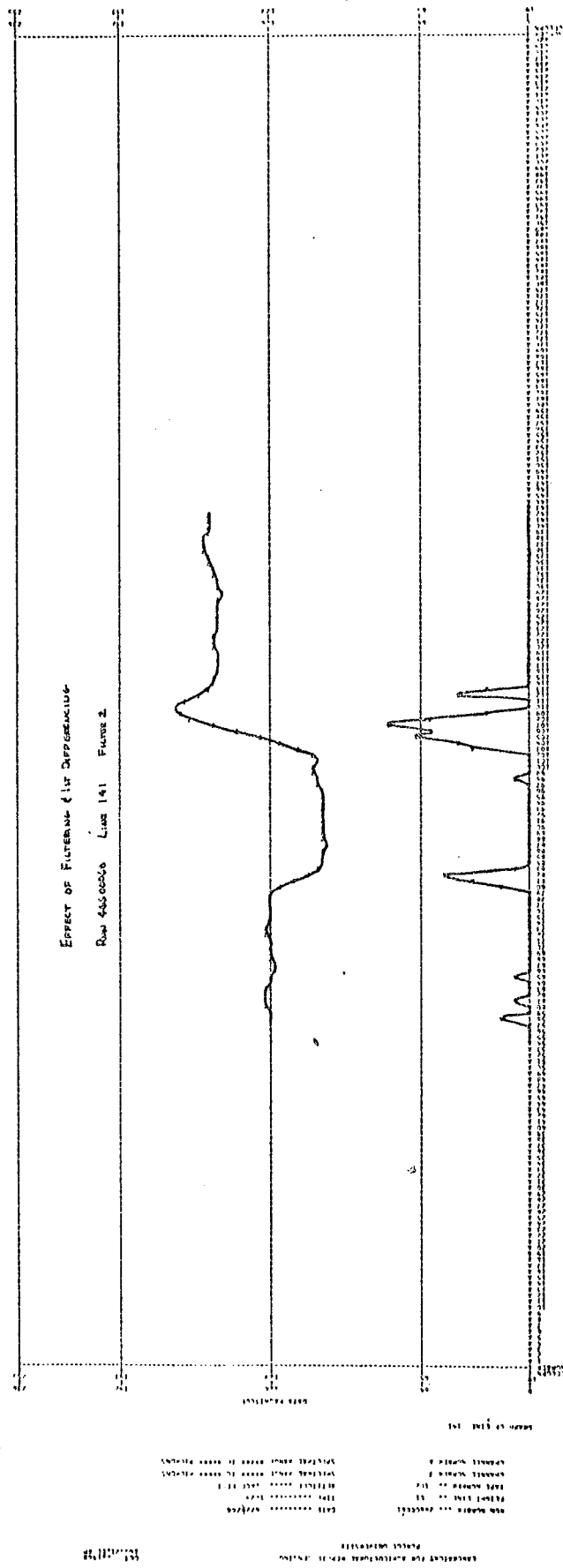


Figure 5e. Filtered IR data line 141

for the small computational cost involved. The filters were programmed and a filtered data tape written for the several flight lines. As a check on the effect of the filter the Fourier transforms of many scan lines were computed before and after filtering. Plots of the magnitude of the frequency domain representation of line 141 from the C1, 1966 flight line are presented in Figure 5b, c for the visible band aperture and thermal IR scanner. Data lines 141 and 221, Figures 5d and e, show the shape after filtering along with the derivative of both. As can be seen, the scanner line has a much smoother contour and the derivative has fewer small amplitude spikes.

Scanner data was preprocessed using these filters and border enhancement was carried out on the altered data. Both differencing and step function approximation to be discussed next used the filtered data as input. The results of the enhancement of imagery will be discussed later in this report.

#### Step Function Approximation

The basic notion behind the step function approach is similar to that for the border detection by differencing approach. It is hypothesized that data values are relatively constant over an agricultural field, pasture, or other areas of homogeneous nature. Changes in the value of the area constant will generally take place at borders and the data is assumed relatively constant in the next area. This hypothesis suggests that a sequence of step functions could be fit to the data lines and columns which would step or jump at borders to new values in successive areas.

The graph of the IR data for line 141 (Figure 3b) suggests the step function nature of certain areas. Examination of many lines and columns



of data led to the design of a basic algorithm which has been under test. The approach to implementing such a scheme was arbitrary and an analytical method of improving the algorithm is being sought.

The logic behind the construction of the present algorithm is as follows: Choose a minimum averaging span of scanner samples and after that set has been averaged, test subsequent points for significant deviations from the average. Since "noise" pulses in the data could cause false jump indications, a minimum is imposed on the number of points which must deviate from the existing average in order that a jump be defined. The jump criterion should be some function of the statistics of the line.

These notions were used as a basis for the step function algorithm. Several parameters are imbedded in the above definitions and none have any associated means of finding their values. Thus once an algorithm is chosen, the problem still remains to find suitable values for the parameters. The parameters can in fact be considered part of the algorithm. The parameters in question for the method suggested above are:

1. The number of samples to be averaged before jumps will be tested for. This would be counted from the sample at which the last jump was defined.
2. The value of deviation which qualifies as a jump.
3. The number of consecutive samples which must deviate from the existing average for a jump to be specified.

These parameters must be specified for the horizontal and vertical dimensions.

The most critical parameter is the jump tolerance. Since no a priori knowledge is available to enable prediction of a jump level,

a reasonably logical approach was chosen. The standard deviation of the line segment being averaged is computed and this quantity is used to set the tolerance for detecting a jump. The choice of this measure for determining the jump tolerance completes the basic definition of the algorithm. It is clearly heuristic and it is intended to serve as a basis for further research on the problem of boundary detection.

Once the structure of the algorithm is defined, operational specifications can be made. The first problem considered was that of specifying the value of the jump tolerance which is to be a function of the standard deviation of the line segment. The choice is a first order nonlinear function. The multiplier is a variable which is determined by a measure of quality of the step function approximation for the entire line. The present measure is the total number of jumps in a line. The reasoning in this choice is that since no error measure is available, a constraint on the number of borders found per line should offer a reasonable step in the direction of optimizing the process. Inspection of the imagery gives an average number of borders per line for a type of area such as grain farm land. By constraining the algorithm to specify this many borders on the average, a more accurate border approximation is expected.

The steps constituting the algorithm are as follows:

1. Compute average for line segment:

$$m_j^K = \frac{1}{j - J_1^K + 1} \sum_{i=J_1}^j X_i$$

$m_j^K$  = the average at the jth column.

$J_1^K$  = the starting column of the current Kth line segment.

$j$  = present column being addressed.

$X_i$  = data value of ith column.

$K$  = the segment indicator.

2. Compute standard deviation of the line segment:

$$\sigma_j^K = \left[ \frac{1}{j - J_1^K + 1} \sum_{i=J_1^K}^j X_i^2 \right]^{1/2} - m_j^K$$

$\sigma_j^K$  = standard deviation at column  $j$  for segment  $K$ .

3. Compute jump tolerance for segment:

$$L_j^K = M_L \sigma_j^K$$

4. Test for jump:

$$\epsilon_j^K = |X_j - m_j^K| \text{ (Deviation from mean)}$$

$$T_j^K = \epsilon_j^K - L_j^K$$

If  $T_j^K$  is positive, define a possible jump at column  $j$ .

$T_j^K$  must remain positive for NJUMPL consecutive samples for jump to be accepted.

5. If a jump is specified at column  $j$ , reset average to zero and begin averaging again at column  $j + 1$  and average for NSPST columns before testing for jump.

6. The multiplier for the jump tolerance ( $M_L$ ) is determined from the previous value and the number of jumps in the present line. If the number of jumps was zero, the multiplier is reduced in value by a given increment and the process repeated for the line. If the number of jumps was greater than NJMPL, the multiplier is increased and the process repeated. This process imposes negative feedback on the algorithm and tends to control the performance. Also the value of the computed tolerance is limited both above and below.

Testing of the algorithm revealed a problem due to wide boundary features - specifically the road in the C1 flight line. The point at which the border should be defined is the middle of the road. However, as the algorithm scans from left to right the road border will be defined on the left side of the road. Similarly in a right to left scan, the border would be defined on the right side of the road. Such conditions could introduce several resolution elements of error. To reduce this error, the algorithm was expanded to include a left scan as well as a right scan of each data line. The results are then examined for border indications which are "close". If two are judged close, they are averaged and the border defined, i.e., the midpoint is taken instead of the two adjacent points.

A simplified block diagram of the algorithm is shown in Figure 6a. This routine searches for boundaries in scanner lines. A similar routine exists in the system for columns. It does not, however, incorporate the

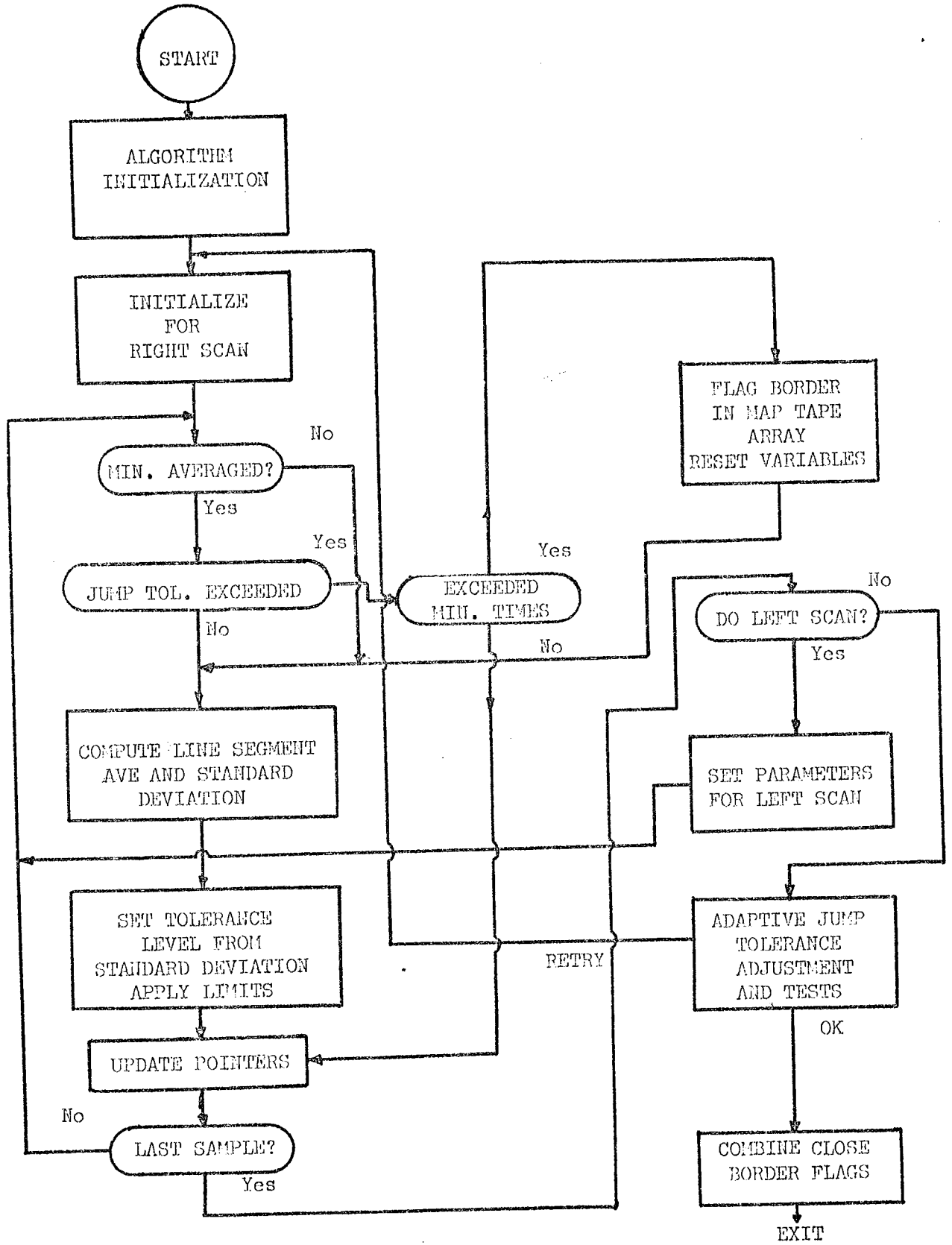


Figure 6a. Step function algorithm

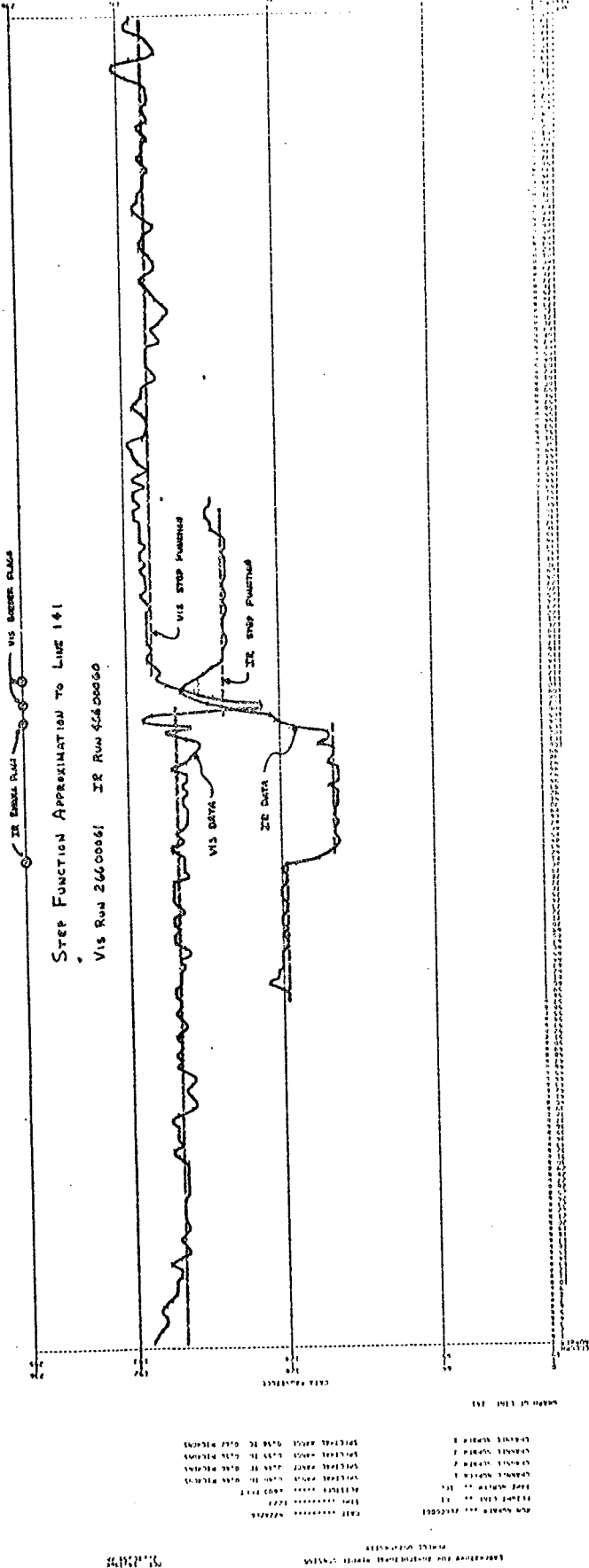


Figure 6b. Step function approximation for line 141

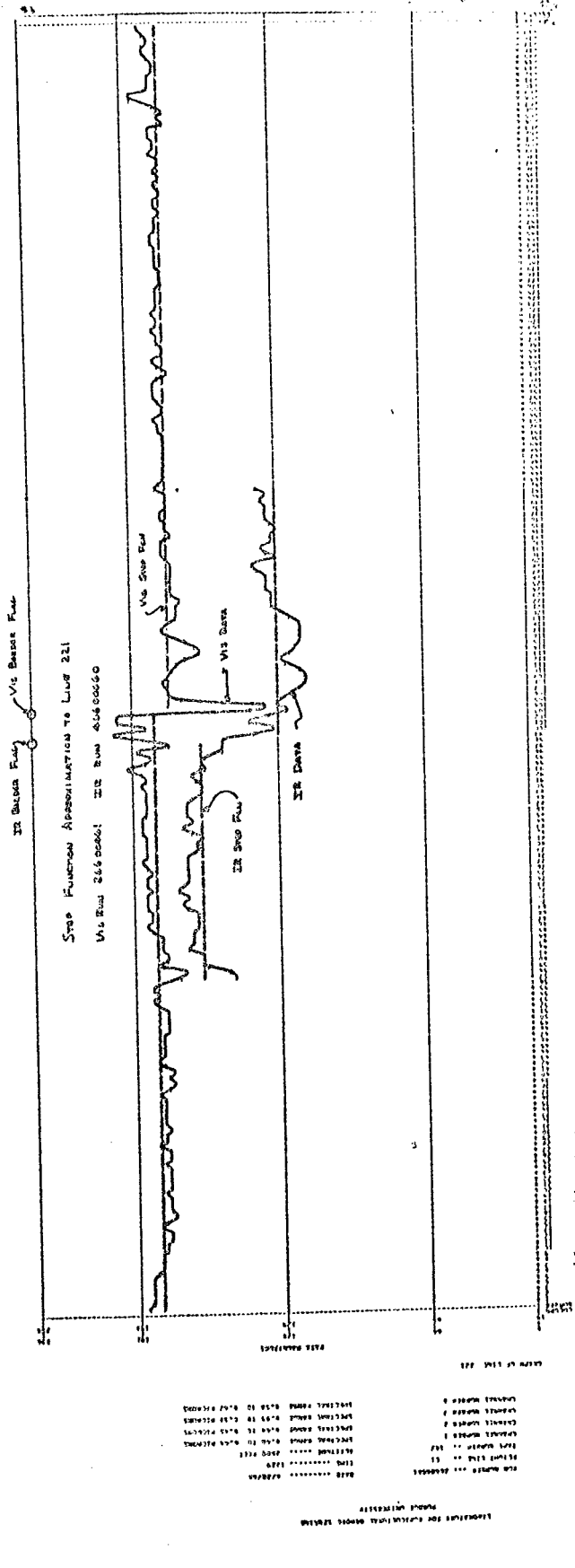


Figure 6c. Step function approximation for line 221

reverse scan feature discussed above. Figures 6b and c contain plots of the step function approximation for lines 141 and 221 discussed earlier. Although the approximation appears good when observing one or two lines, the overall performance for a large area is not adequate for overlay. Further work must be done to improve this scheme. The basic assumptions behind its design appear sound and an approach to optimizing its performance is outlined at the end of this report.

In order to enable experimentation with the difference and step approximated data, a border map tape is formed during border enhancement and cross correlation operations use this tape as input. The ID and data format of this tape is made the same as the LARS data storage tapes so that the LARS pictorial printout program\* can be used as needed to study the border enhanced data. The line and column differences, line and column step function approximations, the line data values, and the sum of the line and column differences for the visible and IR tapes are written on the border map tape in the border enhancement process. This 12 channel tape is used by the correlation program to define checkpoints. A display program is included in the system to pictorially print out the results in a gray-scale mode or a thresholded mode. Also, any two channels can be displayed in the threshold mode with an asterisk for one channel and a plus sign for the other; or if both channels are over the given threshold for the same point, a "B" is printed.

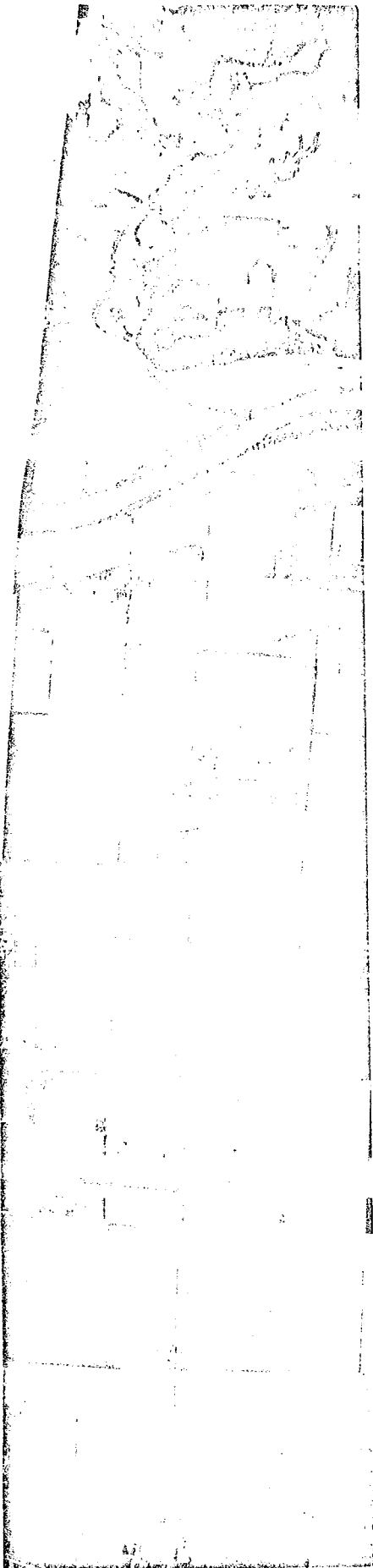
Figure 7a, b, c and d shows thresholded printouts for the sum (horizontal plus vertical) first difference channel of the border map tape for several flight lines. A gray-scale pictorial printout is

\* See LARS Program Abstract DH 112

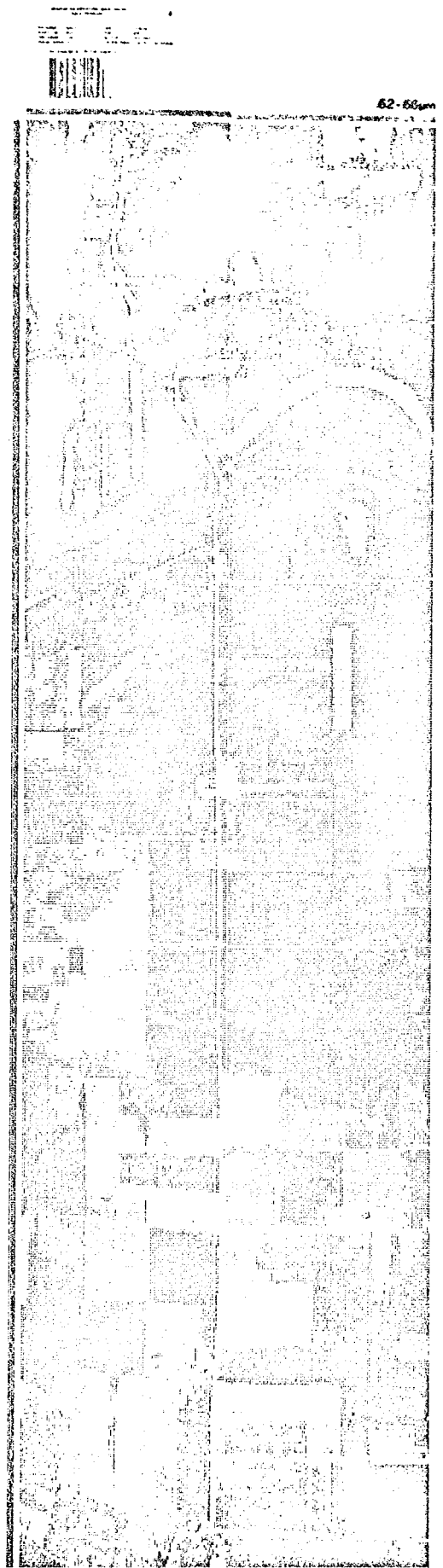
included in the center strip of the figures to display the boundaries as they are seen unaltered. The left strips are thresholded pictorial printouts of the 1st difference values for the visible band aperture. The right strips are thresholded printouts of the IR data. This printout is generated by testing each difference value to see if it exceeds a given threshold value. If it is equal or below a blank is printed. If above an asterisk is printed. In this manner, a border map is produced which defines the representation of the true borders made by the approximation technique. Figure 7a shows a comparison of the computer gray-scale pictorial printout of area C1 and a photograph of the same area. This is included to enable evaluation of the quality of the computer gray-scale and to supply a high resolution display of ground features via the photograph that may not be clearly identifiable in the computer printout.

Figures 7b, c and d are border enhancement by differencing comparisons. In Figure 7b, the most successful border detection was achieved for the county road which runs down the center of the strip, the Wabash river banks which run across the top, and several cross roads and fields throughout the area. Comparison of lines in the border display with field and road edges in the gray scale gives some measure of the quality of the enhancement process. The visible band data has 12 coincident channels to collectively enhance borders whereas the IR band data has only 1 to 4. This factor can be seen in the lower quality of the IR border printout. The center road and riverbank features are less clearly defined than they are in the visible and some field boundaries do not exist which are seen in the visible - and vice versa. The IR enhancement in Figure 7b was made from four coincident channels from the C1 area. Figure 7c and 7d contain comparisons in which the IR was enhanced from one channel (8-14 $\mu$ m). This data is from the Indiana highway 37 flight in





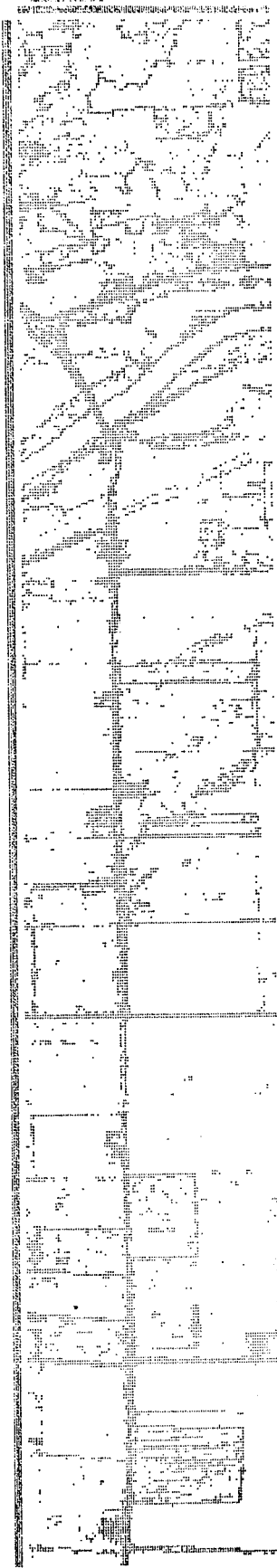
Photograph



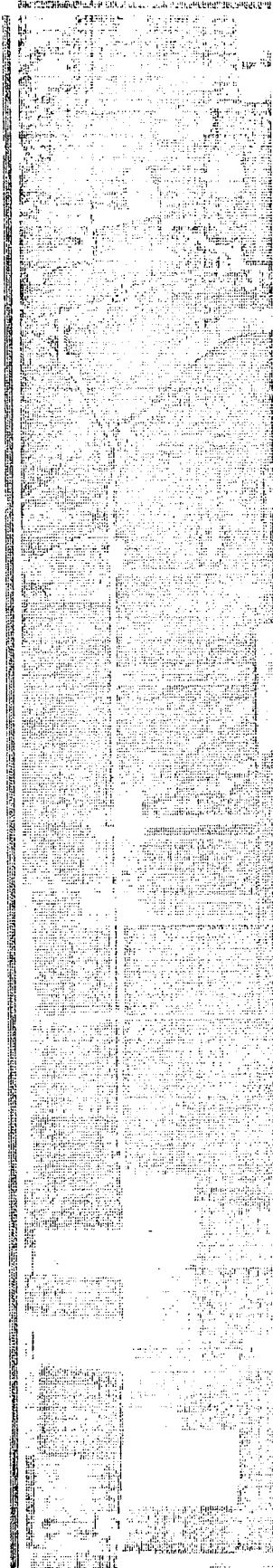
Computer Pictorial Printout

Figure 7a. Flight line PF21

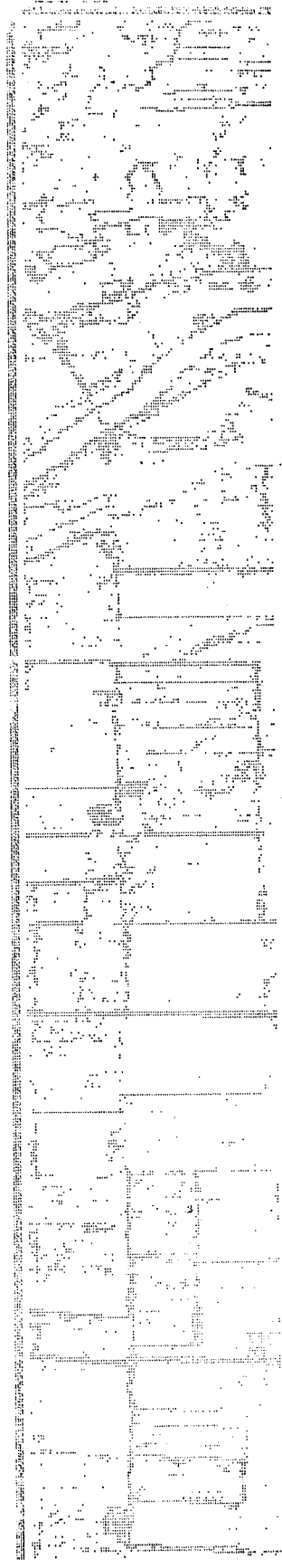
.62-66µm



Visible band borders

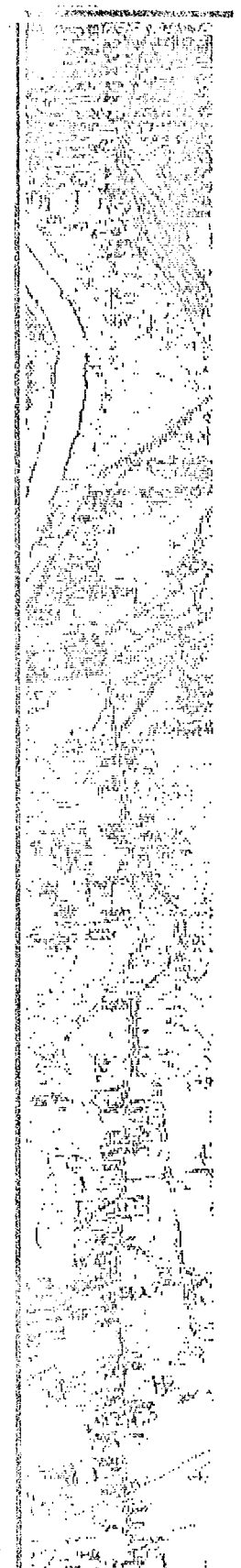
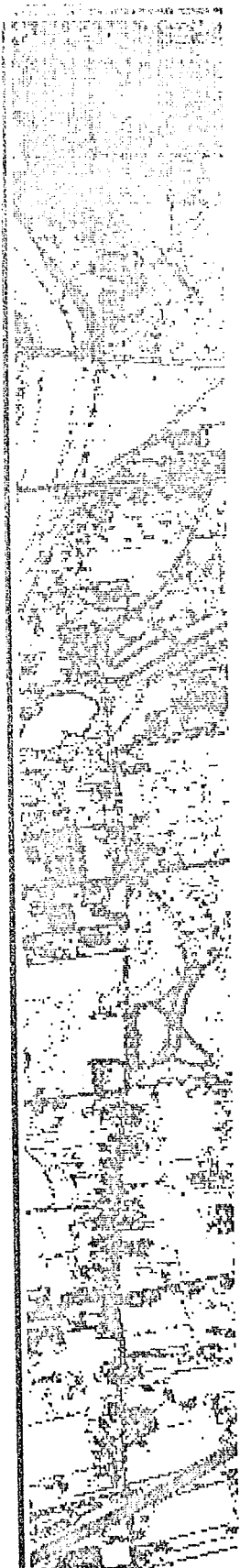
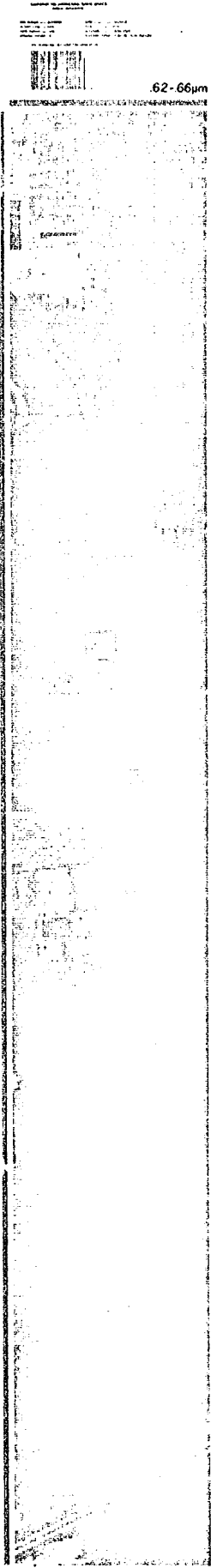


Gray scale



IR band borders

Figure 7b. Border enhancement display  
Flight line PF 21



Visible band borders

Gray scale

IR band borders

Figure 7c. Border enhancement display  
Flight line HW 371



Visible band borders

Gray scale

IR band borders

Figure 7d. Border enhancement display  
Flight line HW372

1967. The 12 channel visible band enhancement is of good quality, however, the IR enhancement is poor and many sharp boundaries in the visible range are not seen at all in the IR. The data overlay problem is the most severe in the case where only one channel is available as would be expected.

Border enhancement using the step function algorithm was not successful enough at the present stage of development to produce relevant border pictorial printouts. One interesting result was obtained, however. The performance of the algorithm was markedly improved when prefiltering was employed. The border map printout was improved from an extremely "noisy" representation to one where about half of the borders were represented accurately with much fewer spurious border points.

Border enhancement map tapes were generated for several runs from two flight lines and cross correlation and overlay was carried out on this data. The results of these operations is discussed in the following sections.

V. Cross-Correlation Process

Part two of the overlay system (See Figure 1) correlates lines and columns from the border tape and defines overlay checkpoints where a definite point of correlation can be found. There are two aspects to the cross correlation process: 1) computing a correlation function and defining a "lockon", and 2) deciding whether or not the lockon is valid and should be used as a checkpoint.

The form of the data to be used for cross-correlation is selected by the program operator. Data value, first difference, or step function representation can be chosen for visible and IR and for horizontal and vertical correlation. The horizontal correlation function is computed for each line and the vertical is computed and averaged for five columns selected from the portion of the flight line where visible and IR data exists.

The correlation function used is the product function:

$$\theta_j = \sum_{i=i}^N x_i y_{i+j} \quad -10 \leq j \leq 10$$

where:  $x_i$  = Visual data point  $i$

$y_{i+j}$  = IR data point  $i+j$

$N$  = Integration range

Correlation function plots for lockon and no lockon conditions for lines and columns for various data forms are shown in Figure 8.

Deciding on the value of a lockon is governed by simple logic based on the known nature of the scanner misalignments. In the present experiments the following conditions must be met by a correction shift value for it to be used as a valid lockon:

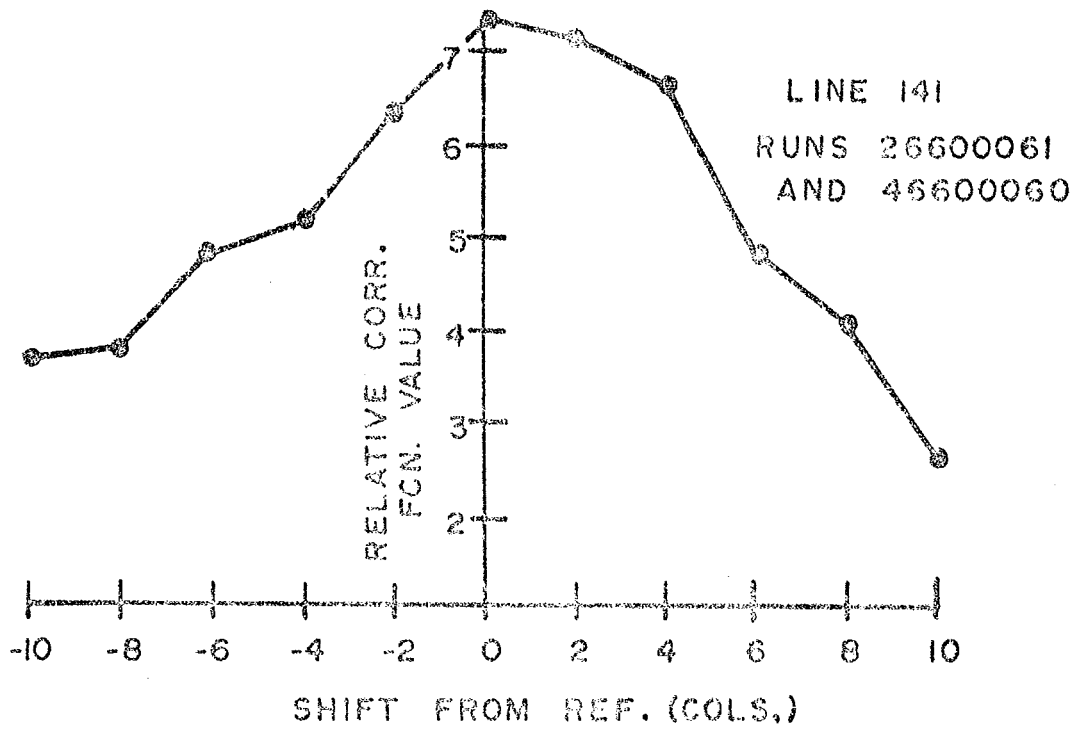


FIGURE 8a. EXAMPLE OF LOCKON CORRELATION FUNCTION FOR A LINE

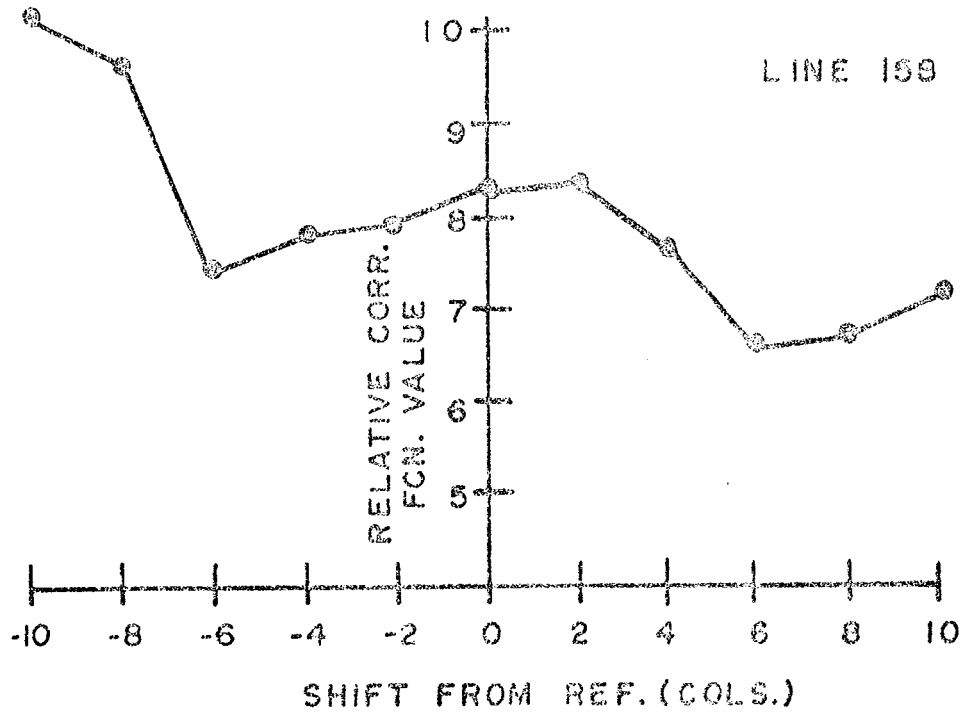


FIGURE 8b. EXAMPLE OF NO LOCKON CORRELATION FUNCTION

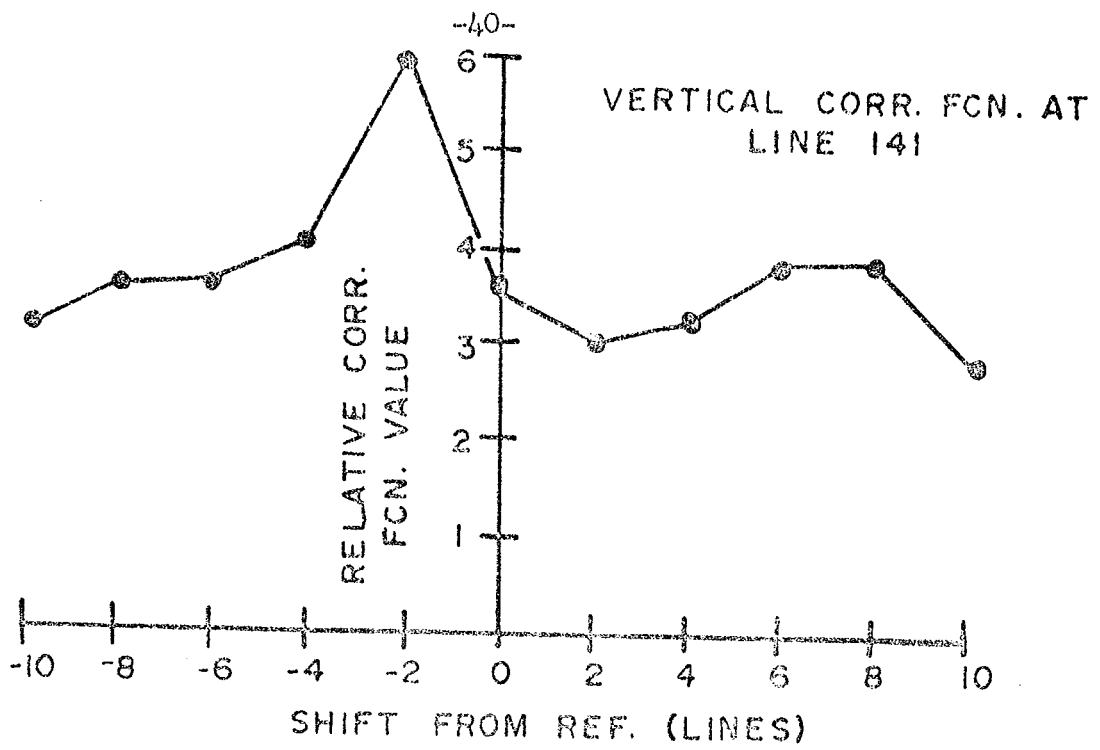


FIGURE 8c, EXAMPLE OF LOCKON CORR. FUNCTION FOR COLUMNS

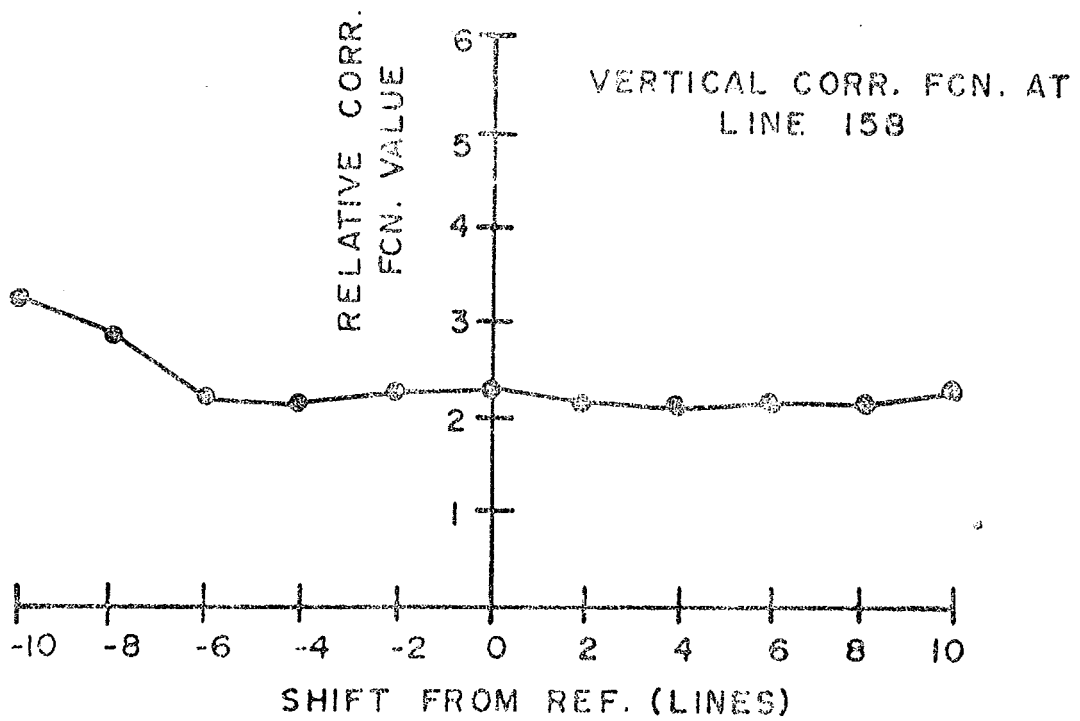


FIGURE 8d. EXAMPLE OF NO LOCKON CORR. FUNCTION FOR COLUMNS



1. The shift values for the last N lines must be within T lines or samples of each other. N is typically 10 and T is 1.
2. The change from the last lockon as defined in (1) no more than 1 different from present value.

A checkpoint is defined; if in addition to the above being true:

1. The present lockon is different from the last.
2. The previous line defined a no lockon condition.
3. At least 20 lines have been processed since last checkpoint.

The checkpoints are computed separately for horizontal and vertical lockons and passed to the overlay part of the system.

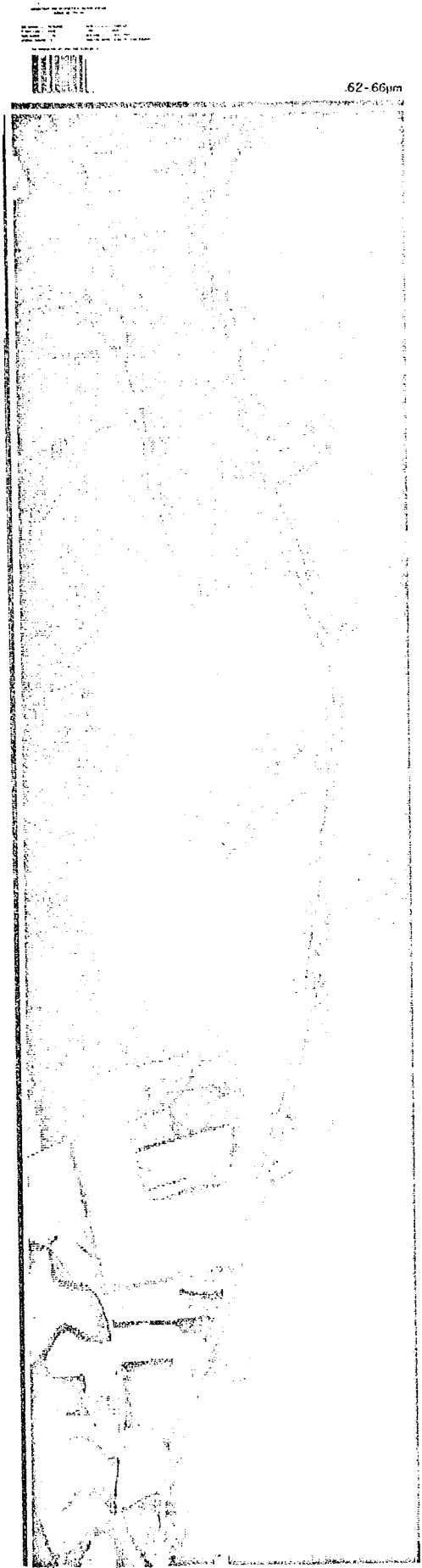
The correlation scheme defined here evolved through experimentation using trial and error plus intuition. The rather severe conditions which are imposed on lockon acceptance were necessary because of the large number of spurious "lockons" which were being observed. Inspection of final results showed these conditions and "smoothing" measures had to be taken to achieve more accurate overlay. More general techniques for judging lockon quality must be developed since the present methods must be considered to be data dependent since they are experimentally developed for a limited amount of data. The correlation process was used to overlay data from several runs as described in the overlay results section.

## VI. Data Overlay Process

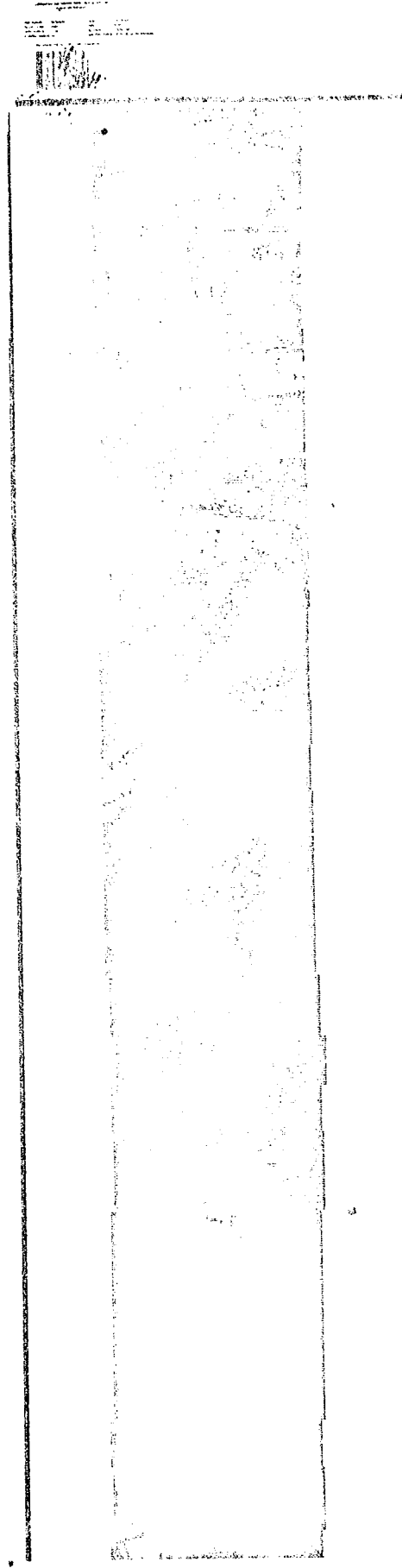
This part of the system carries out the data combination and writes the new overlay data storage tape. It is directed by the initial alignment data read from cards and the checkpoints defined in part two. The functions performed were basically defined in the discussion on overlay details. The present system replaces one or more of the visible channels

by the overlay data forming a new 12 channel tape which is fully compatible with the present data handling system.

An updated version will combine data such that all channels from both the master and slave input tapes will exist on the new or overlay tape. When the new LARS data handling system becomes operational, the overlay system will enable combination of all 17 sensor channels presently available on one tape in geometrical coincidence. An example of the placement of the  $40^{\circ}$  thermal IR channel on the overlay tape is shown in Figure 9 for the 1967 HW372 flight line. The left printout is channel 8 from the visible or master tape with the IR on the right. The results of overlay operations carried out with the present system are discussed next. The preceding discussion was intended as a description of the development process and does not define a final system. Further development work is proposed in a subsequent section.



Visible aperture



IR aperture

Figure 9. Overlay comparison  
Flight line HW372

## VII. Overlay System Results

The present configuration of the overlay system is diagrammed in Figure 10. Border enhancement, cross correlation, and overlay operations can be executed in one job under control of the operator. The scanner data studied was taken from three flight lines as follows:

1. Flight line code C1; covering a seven mile strip south of the Wabash river in south central Tippecanoe County, Indiana. Data taken in June 1966.
2. Flight line code H371,2; selected portions of a 75 mile flight line flown on April 1967, following Indiana Highway 37 which runs from south of Indianapolis to near Bedford, Indiana. The northermost  $2/3$  of the line has been studied in the overlay project (approximately 51 miles).
3. Flight lines PF21 and PF25 from July 1968 flight covering an E-W and N-S strip running full length of Tippecanoe County, Indiana.

The run numbers and lengths of the individual data runs used are shown in Table 1.

Two performance measures for the border enhancement and cross correlation process are used, one is percent lockon for the horizontal and vertical dimensions, and the second is manual overlay accuracy estimation. Computer runs have been made using the three types of input data to the correlation process. Table 2 compares the lockon percentages for the combinations chosen for some of the data tested. Percent lockon is the proportion of the total number of lines in the

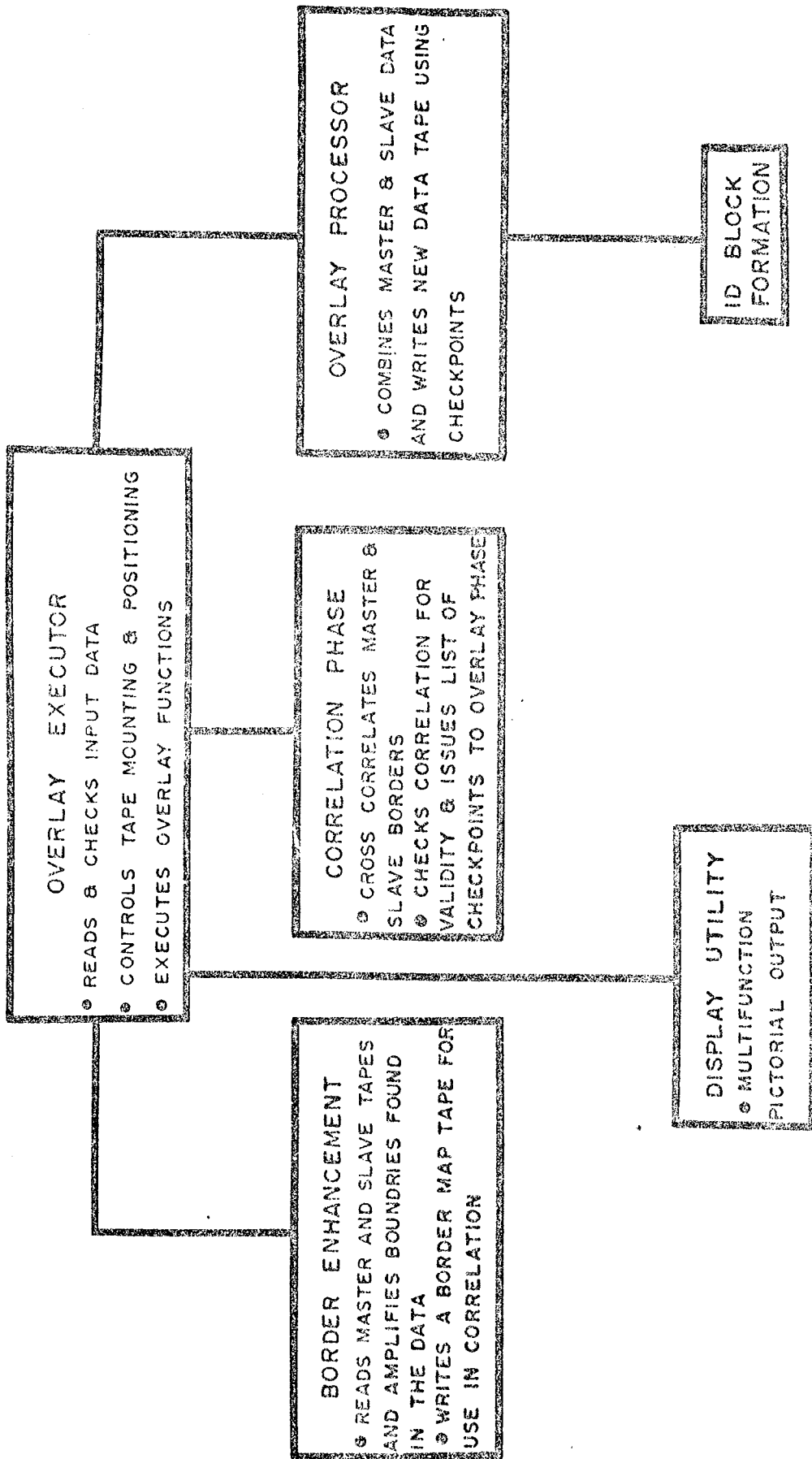


FIGURE 10. LARS OVERLAY SYSTEM

Code	Run Numbers	Scan Lines	Approx. Length (Mi.)	Date Data Taken	Alt. (Ft.)
C1	26600061 (Vis)	949	7	6/28/66	2600
	46600060 (IR)	869	6		
H371	26700010 (Vis)	2661	15	4/28/67	3200
	26700011 (Vis)	1549	9		
	46700010 (IR)	4210	24		
H372	26700021 (Vis)	2449	14	4/28/67	3200
	46700020 (IR)	2449	14		
	26700022 (Vis)	2363	13		
PF 21	26800020 (Vis)	700	7	7/30/68	5000
	16800020 (IR)				
	36800020 (IR)				
	46800020 (IR)				
PF 25	26800030 (Vis)	1100	11	7/30/68	5000
	16800030 (IR)				
	36800030 (IR)				
	46800030 (IR)				

Table 1. Flight lines studied

		Visible Data					
		Data Value	1st Diff.	Step FCN	Data Value	1st Diff.	Step FCN
IR Data	Data Value	.62	1.25	9.35	5.0	1.84	6.05
	1st Diff.	.93	23.05	14.33	.79	59.21	22.89
	Step FCN	10.90	19.31	37.69	19.21	21.58	17.11
		Horizontal			Vertical		

Table 2a. Percent lockon for run C1 (460 lines correlated)  
 Run - 26600061 (Vis)  
 46600060 (IR)

		Visible Data					
		Data Value	1st Diff.	Step FCN	Data Value	1st Diff.	Step FCN
IR Data	Data Value	.09	10.78	7.0	0.0	0.0	1.29
	1st Diff.	20.83	23.93	12.73	0.0	8.78	9.06
	Step FCN	8.70	10.05	35.60	0.1	1.44	12.34
		Horizontal			Vertical		

Table 2b. Percent lockon for HW371 (1128 lines correlated)  
 Run - 26700010 (Vis)  
 46700010 (IR)

run for which the lockon criterion is satisfied. The correlation data types are the two border enhancement processes - differencing and step function; and the third is the unaltered scanner data.

In most cases the first differencing approach is shown to be the best enhancement method for improving the correlation of the visible band and far IR band data. The step function form ranks second in some combinations for a few of the runs. Correlation using the unaltered data values gives very poor performance in almost all combinations.

The quality of the checkpoints defined by the correlation program is difficult to determine since visual matching of pictorial printouts of the data being combined is usually not possible to better than one line and sample and often it is impossible to get even that close. Visual testing of the overlay runs made to date indicates that an average error of about two lines and samples exists. Since the test uncertainty is about 1 unit the actual accuracy is somewhat better than this. The vertical overlay appears to be quite exact and the horizontal overlay generally is about two samples in error, thus contributing the bulk of the overall average of two. Specifically, the error is determined by examining N points in a run visually and estimating as well as possible the line and sample error at that point. The average uses the following error formula:

$$\Sigma_R = \frac{1}{N} \sum_{i=1}^N \left[ \epsilon_{H_i}^2 + \epsilon_{V_i}^2 \right]^{1/2}$$

where:  $\Sigma_R$  = average overlay error for run R

N = number of points in the run examined

$\epsilon_{H_i}$  = the number of samples of overlay error at the ith point



and  $\epsilon_{V_i}$  = the number of lines of overlay error at the ith point.

The value of the error for the runs tested is given in Table 3.

The overlay system is being used in its present developmental form to combine data from the two apertures in response to requests for overlaid data from LARS researchers. Work is in progress to overlay data from the reflective IR aperture which will, when completed, allow feature selection and classification based on visible band, reflective IR, and thermal IR data. Several areas where continued development work is recommended on the general overlay problem are outlined in the next section.

Code	Number of Points Tested	Ave. Error
C1 (1966)	11	2.1
H371 Part 1 (1967)	14	3.1
H371 Part 2 (1967)	8	2.5
H372 Part 1 (1967)	7	3.4
H372 Part 2 (1967)	11	2.9
PF21 (1968)	5	1.9
PF25 (1968)	7	1.2

Table 3. Overlay Error

VIII. Further Studies

Several new lines of investigation have begun on the overlay study. The first is an exploration of the utility of the two dimensional Fourier transform for feature enhancement and cross correlation. There are two aspects to this process, 1.) Possible simplification of the computation of the cross correlation function by multiplying the transforms of the data sets in the frequency domain and taking the inverse transform to get the cross correlation function. 2.) Frequency domain processing of features by filtering.

The frequency domain computing of the correlation function is possible as shown below. Let  $\{x_i\}$  and  $\{y_i\}$  be sets of data points for which the cross correlation function is to be computed. The desired function is:

$$\phi_{xy}(j) = \sum_{i=1}^N x_i y_{i+j} \quad -N + 1 \leq j \leq N - 1$$

The discrete Fourier transform of this function is:

$$FT(\phi_{xy}(j)) = \frac{1}{N} \sum_{j=0}^{N-1} \left( \sum_{i=1}^N x_i y_{i+j} \right) e^{-\frac{\sqrt{-1} 2\pi k j}{N}}$$

Let  $p = i + j, \quad j = p - i$

Then:

$$FT(\phi_{xy}(j)) = \frac{1}{N} \sum_{p=0}^{N-1} \sum_{i=1}^N x_i y_p e^{+\frac{\sqrt{-1} 2\pi k i}{N}} e^{-\frac{\sqrt{-1} 2\pi k p}{N}}$$

or:

$$\Phi_{xy}(k) = \Phi_x(k) \Phi_y(-k)$$

where the  $\Phi_x$  denotes the transform of x

Then the inverse transform of  $\Phi_{xy}$  gives the cross correlation function:

$$\phi_{xy}(j) = \sum_{k=0}^{N-1} \Phi_{xy}(k) e^{\frac{\sqrt{-1} 2\pi k j}{N}}$$

Thus if the total computation time for the frequency domain method using the Fast Fourier Transform algorithm is less than the time for computing the lagged product of the two sequences the method has value. It is not obvious that it will be faster.

Some work has been done toward developing frequency domain processing capability for two dimensional arrays. The major problem at present is to find a method of transforming large arrays using the fast Fourier transform routine using the limited core space available at LARS. The work of Cooley (Ref. 4) and Oppenheim (Ref. 7) are major inputs to the image processing work proposed.

Another problem on which study is beginning is that of measuring the error in boundary detection algorithms. Since the processes are intended to find field and road boundaries, the obvious way to test performance is to compare estimated boundaries to true boundaries. Thus a true border map tape is being formed by picking out borders from scanner data pictorial printouts and punching the coordinates of line segment ends into cards. A program being written will read these cards and write line segments denoting borders on tape along with scanner data from one or more channels. Once one or more true border tapes are available, a numerical measure of border enhancement accuracy can be obtained. Then some optimizing scheme can be employed which will act to modify the algorithm such that the border enhancement error is minimized.

Let B be the set of true borders in some area A and let  $F_B$  be the set of approximate borders defined by, for example, the step function curve fit algorithm. Then the goal of the investigation is to find a means of minimizing the error:

$$\Sigma_A = [B - F_B] \text{ over the area A.}$$

The error measure is not defined by the above expressing, however.

Specifically let  $B_{V_{ij}}$  be the column position of the jth vertical border point in the ith line. Let  $B_{H_{ij}}$  be the jth horizontal border point in the ith line. The two dimensions are defined because the system approach stated above is to correlate in two orthogonal dimensions and border error will therefore be studied in these two dimensions. The border approximation will be denoted as  $F_{B_{H_{ij}}}$  and  $F_{B_{V_{ij}}}$ . Then horizontal and vertical quantitative errors are  $F_{B_{H_{ij}}}$  and  $F_{B_{V_{ij}}}$  defined as:

$$\epsilon_{H_i} = \sum_{j=1}^N |B_{H_{ij}} - F_{H_{ij}}| \text{ where } j \text{ is the } j\text{th border in line } i$$

N is the number of border points in the line.

$$\epsilon_{V_j} = \sum_{i=1}^M |B_{V_{ij}} - F_{V_{ij}}| \text{ where } \epsilon_{V_j} \text{ is the border error for the } j\text{th}$$

column which is obtained by summing down the column from line  $i^s = 1$  to line  $i = M$ .

These expressions give the border error in columns and lines over and area A. The border approximation algorithms produce "spurious" borders which do not match or are not close to a true border. For these cases the linear error measure seems inappropriate since there may be no corresponding true point to move the spurious point toward.

Thus approximate border points lying more than a given distance from a true point will be flagged as a "bad border" and accounted for separately. The optimization scheme must then eliminate all bad borders first then minimize the linear error over the entire area.

As part of the step function border algorithm study a comparison will be made with the border approximation obtained by using the least squares spline function technique. In this method a set of polynomial functions are fitted to segments of the data. The segments are called splines and the points at which adjacent segments meet are called knots. The work of Rice and deBoor (Ref. 6) is being used as primary reference. Their algorithm generates cubic splines with fixed knots and has a facility for seeking optimum knots. It will be used to approximate borders over the same area as the overlay system step function (0 order) algorithm to determine whether or not the least squares approximation offers an improvement in border accuracy over an optimized LARS method.

Other aspects of scanner data improvement, such as yaw angle correction, compensation for scanner look angle effect, data filtering, data compression, and temporal overlay, have been considered but no work has been done on them.

## IX. Summary and Conclusions

This report describes a LARS system development effort to construct a data handling system for automatically correlating and combining scanner data from different apertures. In order to improve the quality of image correlation an image enhancement process was developed which amplifies borders, thereby giving the correlation process improved points which it can lock on. Data is combined using

alignment points generated by the enhancement and correlation process. Data from 7 runs was combined and the average overlay error was 2.5 resolution elements.

Experiments showed that first differencing of the scanner imagery offered the most reliable medium accuracy method of enhancing borders for cross correlation. Low pass filtering of the data did not significantly improve the reliability or the accuracy of this method. A step function curve fitting method for finding borders was experimented with and promises high accuracy border detection if it can be made stable. Pre-filtering of the imagery showed marked improvement in the performance of the step function algorithm. Further work is recommended on this scheme.

A complete overlay program exists which can be used for operational combination of data or for further research. Flexibility has been designed into the system so that the various methods of border enhancement and correlation can be selected by the operator at run time. A general purpose display program is included which can produce either gray scale or thresholded printouts of imagery which has been processed by the enhancement program. A document describing the system is planned.

References

1. J. W. Cooley, J. W. Tukey, "An Algorithm for the Machine Calculation of Complex Fourier Series", Mathematics of Computation, Vol. 19, No. 90, (1965), pp. 297-301.
2. R. W. Hamming, "Numerical Analysis for Scientists and Engineers", McGraw Hill, New York, 1962.
3. W. M. Gentleman, G. Sande, "Fast Fourier Transforms for Fun and Profit", Proceedings of the Fall Joint Computer Conference, (1966), San Francisco, California.
4. J. W. Cooley, P. A. Lewis, P. D. Welch, "The Fast Fourier Transform Algorithm and its Applications", IBM Research Report RC 1743, IBM Watson Research Center, Yorktown Heights, New York, February 9, 1965.
5. J. W. Cooley, "Applications of the Fast Fourier Transform Method", Proceedings of the IBM Scientific Computing Symposium, T. J. Watson Research Center, Yorktown Heights, New York.
6. C. de Boor, J. R. Rice, "Least Squares Cubic Spline Approximation I, II", Computer Science Department Report CSD TR 20, 21, Purdue University, West Lafayette, Indiana, April 1968.
7. A. V. Oppenheim, R. W. Schafer, T. G. Stockham, "Nonlinear Filtering of Multiplied and Convolved Signals", Proceedings of the IEEE, Vol. 56, No. 8, August 1968, pp. 1264-1291.
8. M. B. Dobrin, "Optical Processing in the Earth Sciences", IEEE Spectrum, September 1968, pp. 59-66.
9. G. C. Cheng, R. S. Ledley, "A Theory of Picture Digitization and Applications", Pictorial Pattern Recognition, Thompson Book Co., Washington D.C., 1968, pp. 329-352.
10. J. L. Pfaltz, J. W. Snively, Jr., A. Rosenfeld, "Local and Global Picture Processing by Computer", *ibid*, pp. 353-371.
11. A. Rosenfeld, J. L. Pfaltz, "Sequential Operations in Digital Picture Processing", J. Association for Computing Machinery 13, 1966, pp. 471-494.
12. R. Bracewell, "The Fourier Transform and Its Applications", McGraw Hill Book Co., New York, 1965.
13. G. C. Cheng, "Fundamentals of Picture Digitization", NBR Report No. GC 6606, National Biomedical Research Foundation, Silver Spring, Md., June 1966.
14. "Images Enhanced", IBM Computing Report, May 1968, pp. 3-6.
15. C. A. Brown, J. D. Pardee, "Data Correlation Project Report for Course No. EE 576 - Fundamentals of Signal Description," Purdue University, January 24, 1968.